Molecular Therapy
Original Article

Circular mRNA-based TCR-T offers a safe and effective therapeutic strategy for treatment of cytomegalovirus infection

Lianghua Shen,[1,2,5] Jiali Yang,[3,5] Chijian Zuo,[3] Jian Xu,[1,2] Ling Ma,[1,2] Qiaomei He,[1] Xiao Zhou,[1] Xiaodan Ding,[1] Lixiang Wei,[3] Suqin Jiang,[3] Luanluan Ma,[3] Benjia Zhang,[3] Yuqin Yang,[1] Baoxia Dong,[1] Liping Wan,[1] Xueying Ding,[2] Ming Zhu,[4] Zhenhua Sun,[3] Pengran Wang,[1,2] Xianmin Song,[1,2] and Yan Zhang[1,2]

[1]Department of Hematology, Shanghai General Hospital, Shanghai JiaoTong University School of Medicine, Shanghai 201620, China; [2]Engineering Technology Research Center of Cell Therapy and Clinical Translation, Science and Technology Committee of Shanghai Municipality, Shanghai 200080, China; [3]Suzhou CureMed Biopharma Technology Co., Ltd, Suzhou 215125, China; [4]KuaiXu Biotechnologies Co., Ltd, Shanghai 201315, China

Circular mRNA (cmRNA) is particular useful due to its high resistance to degradation by exonucleases, resulting in greater stability and protein expression compared to linear mRNA. T cell receptor (TCR)-engineered T cells (TCR-T) represent a promising means of treating viral infections and cancer. This study aimed to evaluate the feasibility and efficacy of cmRNA in antigen-specific-TCR discovery and TCR-T therapy. Using human cytomegalovirus (CMV) pp65 antigen as a model, we found that the expansion of pp65-responsive T cells was induced more effectively by monocyte-derived dendritic cells transfected with pp65-encoding cmRNA compared with linear mRNA. Subsequently, we developed cmRNA-transduced pp65-TCR-T (cm-pp65-TCR-T) that specifically targets the CMV-pp65 epitope. Our results showed that pp65-TCR could be expressed on primary T cells for more than 7 days. Moreover, both *in vitro* killing and *in vivo* CDX models demonstrated that cm-pp65-TCR-T cells specifically and persistently kill pp65-and HLA-expressing tumor cells, significantly prolonging the survival of mice. Collectively, our results demonstrated that cmRNA can be used as a more effective technical approach for antigen-specific TCR isolation and identification, and cm-pp65-TCR-T may provide a safe, non-viral, non-integrated therapeutic approach for controlling CMV infection, particularly in patients who have undergone allogeneic hematopoietic stem cell transplantation.

INTRODUCTION

Circular mRNA (cmRNA) is a covalently closed single-stranded structure, offering advantages over linear mRNA, including resistance to exonuclease-mediated degradation and durable protein expression.[1–5] Unlike most linear mRNA that relies on 5′-cap structure to initiate efficient translation, cmRNA instead relies on cap-independent translation elements.[3] A previous study has shown that the median half-life of cmRNA is at least 2.5 times longer than that of linear mRNA in mammalian cells.[6] Several *in vitro* strategies for cmRNA synthetization have been previously reported.[7] Recently, we developed a new group I intron self-splicing system-based system for industrial-scale cmRNA production without the induction of extraneous exon sequences.[8] This system showed high circularization effectiveness and purity, minimized immunogenicity, and strong protein expression *in vitro* and *in vivo*. This novel cmRNA platform has great potential not only for vaccines development but also for mRNA-based therapeutics.

Over the past decade, chimeric antigen receptor T cell (CAR-T) therapies have achieved significant success in the treatment of blood cancers.[9,10] Unlike CAR-T cells that bind to cell surface antigens, TCR-T cells recognize peptides derived from both surface and intracellular proteins that are presented by major histocompatibility complex (MHC) molecules on the cell surface, enabling a broader range of antigen recognition than CAR-T.[11,12] Previous studies have shown that even one single peptide-MHC complex on the target cells can trigger T cell activation, making TCR-T cells are more sensitive to antigens than CAR-T cells.[13,14] Autogenous monocyte-derived dendritic cells

Received 3 July 2023; accepted 10 November 2023;
https://doi.org/10.1016/j.ymthe.2023.11.017.

[5]These authors contributed equally

Correspondence: Yan Zhang, Department of Hematology, Shanghai General Hospital, Shanghai Jiao Tong University School of Medicine, No. 100 Haining Road, Shanghai 200080, China.
E-mail: yan.zhang19510@shgh.cn
Correspondence: Chijian Zuo, Suzhou CureMed Biopharma Technology Co., Ltd., Suzhou 215000, China.
E-mail: zuocj@purecell.group
Correspondence: Zhenhua Sun, Suzhou CureMed Biopharma Technology Co., Ltd., Suzhou 215000, China.
E-mail: sunzh@purecell.group
Correspondence: Pengran Wang, Department of Hematology, Shanghai General Hospital, Shanghai Jiao Tong University School of Medicine, No. 100 Haining Road, Shanghai 200080, China.
E-mail: prwang_sh@163.com
Correspondence: Xianmin Song, Department of Hematology, Shanghai General Hospital, Shanghai Jiao Tong University School of Medicine, No. 100 Haining Road, Shanghai 200080, China.
E-mail: shongxm@shjt.edu.cn

Please cite this article in press as: Shen et al., Circular mRNA-based TCR-T offers a safe and effective therapeutic strategy for treatment of cytomegalovirus infection, Molecular Therapy (2023), https://doi.org/10.1016/j.ymthe.2023.11.017

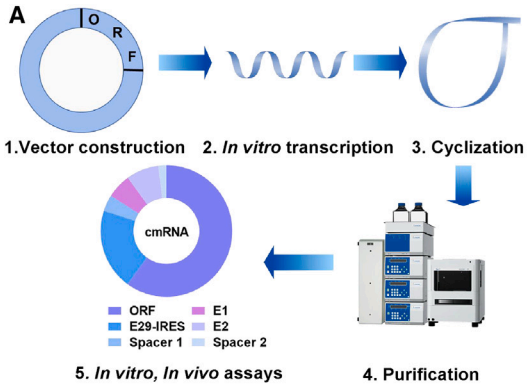

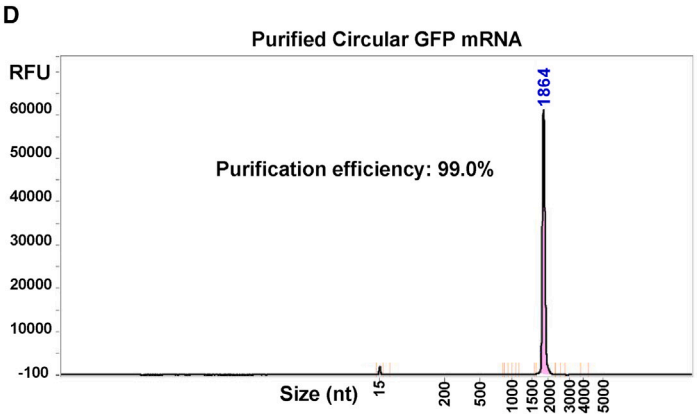

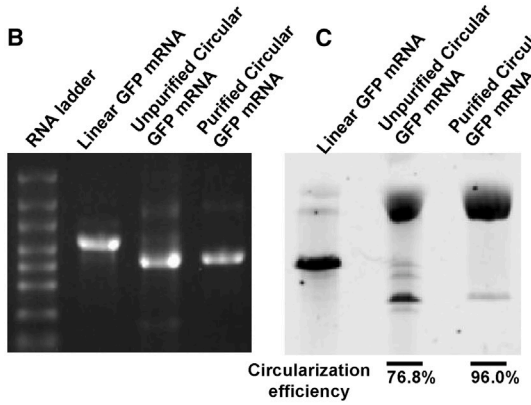

Peak	Size (nt)	Concentration (ng/ul)	RFU	Relative Percent (%)
1	15 (LM)	0.7597	1889	-
2	32	1.2702	109	0.3
3	865	0.1183	56	0.0
4	958	0.3102	65	0.1
5	1120	0.1794	57	0.0
6	1651	0.6353	297	0.2
7	**1864**	**380.4236**	**61285**	**99.0**
8	2504	0.3023	62	0.1
9	2682	0.3691	79	0.1
10	4113	0.7031	110	0.2

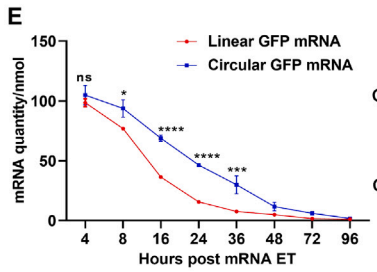

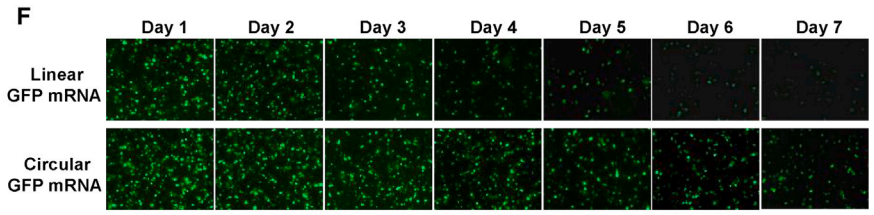

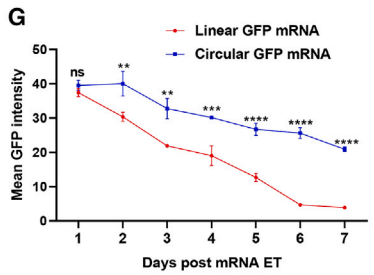

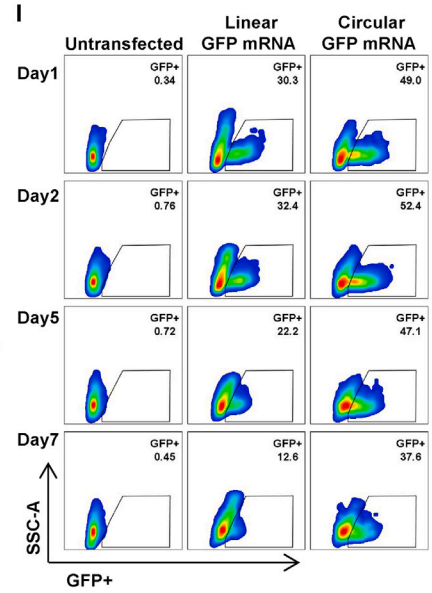

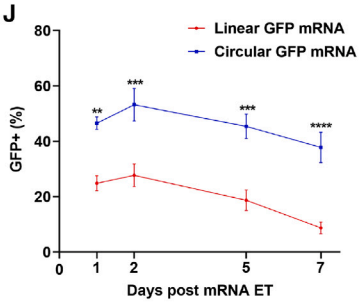

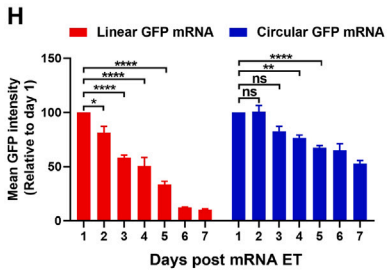

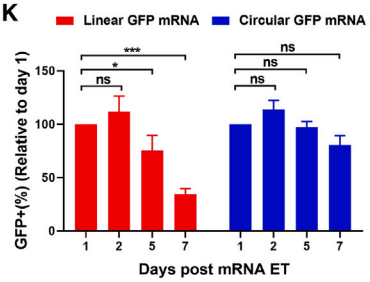

(legend on next page)

Please cite this article in press as: Shen et al., Circular mRNA-based TCR-T offers a safe and effective therapeutic strategy for treatment of cytomegalovirus infection, Molecular Therapy (2023), https://doi.org/10.1016/j.ymthe.2023.11.017

(moDCs) transfected with linear mRNA encoding candidate antigens have been shown to prime and expand the antigen-specific T cells *in vitro*.[15–17] However, validating neoantigens and isolating antigen-specific TCRs remain technically challenging, partially due to the relatively short lifetime of antigen-encoding linear mRNAs in moDCs. It has not been investigated whether antigen-encoding cmRNA can prolong the expression of antigens in moDCs and enhance antigen-specific T cell expansion. In addition, most CAR-T or TCR-T therapies presently use lentiviral or γ-retroviral vectors, and safety concerns still exist.[18] Recently, CRISPR-mediated gene delivery approaches have been developed to produce non-viral CAR-T cells.[19] Both viral-based and CRISPR-based approaches cause genome integration, and the potential long-term side effects need to be carefully evaluated. Currently, there is a lack of *in vivo* studies testing cmRNA-transduced TCR-T cells in the killing of antigen-expressing target cells.

Cytomegalovirus (CMV) infection is one of the most common causes of mortality after allogeneic hematopoietic stem cell transplantation (allo-HSCT).[20] Here, we found that autogenous moDCs transfected with CMV-pp65 cmRNA prime and expand pp65-responsive $CD8^+$ T cells more efficiently than that transfected with linear mRNA. Subsequently, cmRNA-transduced pp65-TCR-T (cm-pp65-TCR-T) cells were shown to efficiently and specifically killed the tumor cells expressing the pp65 antigen and respective HLA *in vitro*. Notably, a twice-monthly administration of cmRNA-pp65-TCR-T cells persistently protected immunodeficient mice from pp65-expressing tumor cells challenge. Collectively, our study demonstrates the great potential of cmRNA in either antigen-specific TCRs isolation and identification, as well as non-viral, non-integration TCR-T therapies against CMV infection after HSCT.

RESULTS

cmRNAs prolong the expression of target proteins in human moDCs

We recently developed a clean-PIE strategy (Figure 1A) for generating cmRNA with high purity (96.0%) and cycling rate (99.0%) (Figures 1B–1D). To compare the duration and expression intensity of cmRNA vs. linear mRNA, we transiently transfected the same amount of linear or circular GFP-mRNA under the same transfection conditions in autologous moDCs from healthy donors. Next, we performed qPCR to detect GFP mRNA levels in moDCs at different time points after transfection of linear or circular GFP mRNA. As shown in Figure 1E, the linear mRNA and cmRNA groups showed similar mRNA levels at 4 h post-transfection, but the elimination rate of circular GFP mRNA was significantly slower than that of the linear mRNA group at 8–32 h post-transfection. In addition, immunofluorescence results showed that transfection of the same amount of circular GFP mRNA resulted in longer GFP expression compared with linear GFP mRNA (Figures 1F and 1G). Seven days after transfection of circular GFP mRNA, the GFP expression level was still about 70% of that at day 1, whereas the moDCs transfected with linear GFP mRNA was only about 20% of that at day 1 (Figure 1H). The western blot results also demonstrated that the GFP expression duration of circular GFP mRNA was longer than that of linear GFP mRNA (Figures S1A and S1B). Subsequently, we further investigated the difference in intensity and duration of linear vs. circular GFP mRNA expression in moDCs by flow cytometry. As shown in Figures 1I and 1J, 24 h after transfection, about 50% of moDCs transfected with cmRNA exhibited GFP expression, while only around 30% of GFP-positive moDCs were observed when transfected with linear mRNAs. Moreover, the GFP signal was still detected in approximately 37.6% of moDCs transfected with cmRNA 7 days after transfection, whereas in the linear GFP mRNAs group, the percentage of GFP-positive moDCs had decreased to 12.6%. Our results showed that the duration of expression and the mean fluorescence intensity of GFP proteins (Figures 1I, 1J, and S1C) were longer and higher in moDCs transfected with circular GFP mRNAs than those transfected with linear GFP mRNAs. In addition, 7 days after transfection of GFP-cmRNA, the expression level was still about 80% of relative to the first day, while moDCs transfected with linear GFP mRNAs had only about 30% (Figure 1K). These results demonstrate that cmRNAs sustain high expression of target proteins, and moDCs transfected with antigen-encoding cmRNAs may serve as a stable antigen-presenting cells to prime and expand antigen-specific T cells *in vitro*.

cmRNA enables efficient screening of pp65 antigen-specific TCRs *in vitro*

CMV infection is an important cause of morbidity and mortality in patients with allogeneic HSCT, in which the expression of CMV-pp65 showed a significant correlation with CMV viral replication (Figures S2A and S2B). We then performed cmRNA-based *in vitro* screening to identify TCRs against CMV-pp65 antigen presented by HLA-A*02:01, HLA-A*11:01, and HLA-A*24:02, the three most common type I-HLA alleles in the Chinese population. We co-cultured $CD8^+$ T cells from healthy donors carrying the

Figure 1. Production process and *in vitro* expression efficiency assay of cmRNA

(A) A novel cmRNA formation strategy for Clean-PIE; agarose-gel electrophoresis (B) and urea-PAGE (C) experiments were performed to analyze the circularization efficiency of PIE of GFP cmRNA. (D) Capillary electrophoresis experiments were used to analyze the percentage of circular GFP mRNA, and the specific values are listed in the table below the figure. (E) The quantity of linear or circular GFP mRNA was determined by RT-qPCR at 4, 8, 16, 24, 36, 48, 72, and 96 h after electroporation (n = 3). (F) GFP expression was assessed from day 1 to day 7 by fluorescence imaging using a fluorescence microscope. The exposure time was constant at 1 s and the exposure intensity was constant at 100%. (G) Quantification of mean GFP expression from day 1 to day 7 by ZEISS ZEN software (n = 3). (H) The mean GFP expression levels relatives to day 1 were counted for the linear GFP mRNA and circular GFP mRNA groups, respectively (n = 3). (I) linear GFP mRNA or circular GFP mRNA was electrotransfer moDCs followed by continuous GFP Flow cytometry detection. (J) Comparison of GFP% at days 1, 2, 5, and 7 after circular or linear GFP-mRNA electrotransfer (n = 3). (K) The GFP expression levels at days 1, 2, 5 and 7 relatives to day 1 were counted for the linear GFP mRNA and circular GFP mRNA groups, respectively (n = 3). All data represent the mean ± SEM. ns, no significant difference,"*p < 0.05, **p < 0.01, *** < 0.001, ****p < 0.0001.

Please cite this article in press as: Shen et al., Circular mRNA-based TCR-T offers a safe and effective therapeutic strategy for treatment of cytomegalovirus infection, Molecular Therapy (2023), https://doi.org/10.1016/j.ymthe.2023.11.017

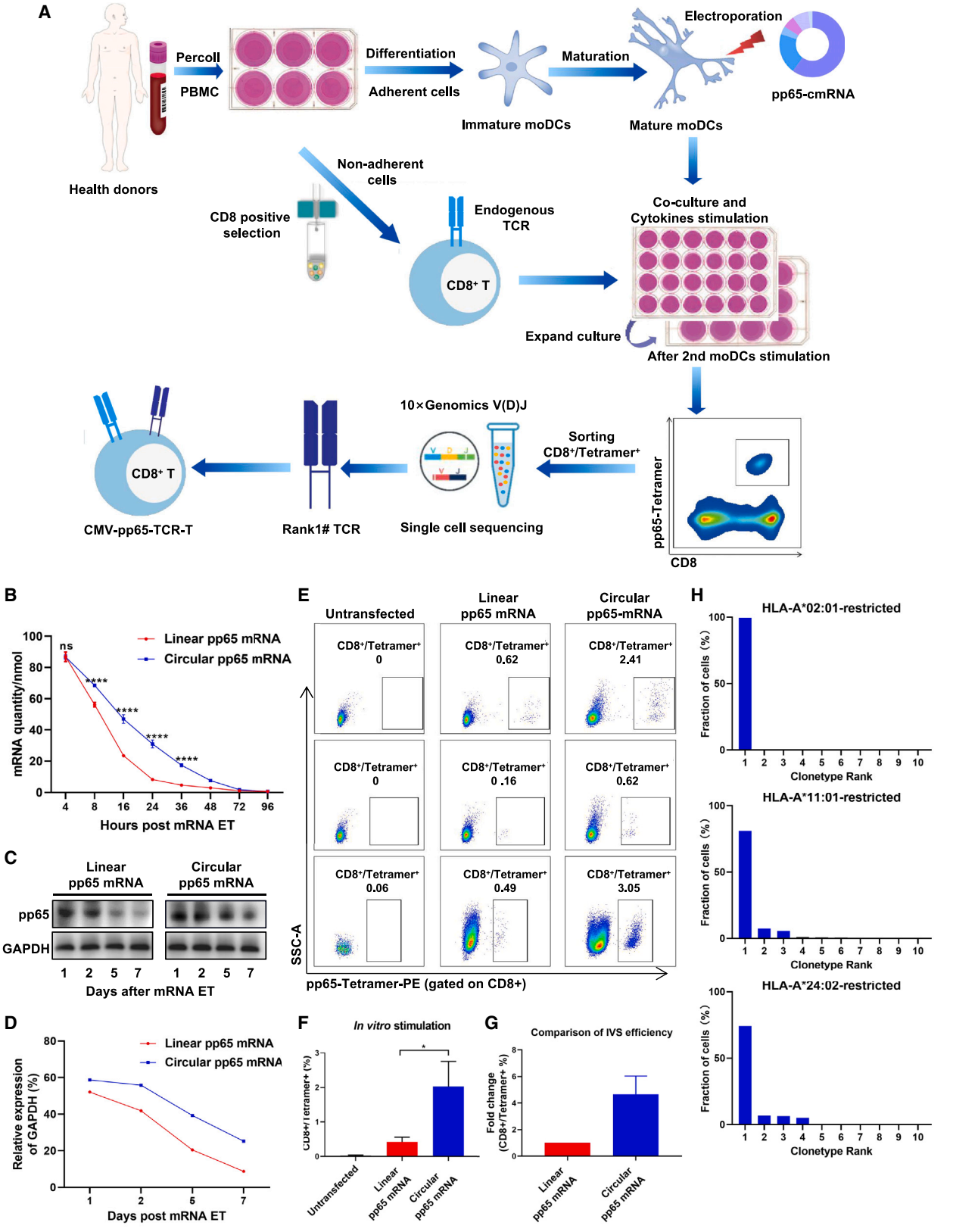

(legend on next page)

HLA-A*02:01, HLA-A*11:01, or HLA-A*24:02 alleles with autologous moDCs transfected with linear or circular pp65 mRNAs. After two rounds of co-culture with freshly prepared moDCs transfected with linear or circular pp65 mRNA at days 0 and 7, we harvested total T cells at day 14, and analyzed pp65-antigen-specific $CD8^+$ T cells using CMV-pp65-tetramer staining (Figure 2A). To determine the translation efficiency of circular or linear CMV-pp65 mRNA, we transfected equal amounts of circular or linear CMV-pp65 mRNA into moDCs cells and quantified pp65 mRNA at different time points by RT-qPCR. The qPCR results indicated that the decay rate of cmRNA in moDCs within 36 h of transfected was significantly lower than that of the linear mRNA group (Figure 2B). We next assessed the protein expression of pp65 in moDCs cells by western blot and mass spectrometry (MS) sequencing, and the results showed that the intensity and duration of pp65 expression of circular pp65 mRNA were superior to that of the linear pp65 mRNA in moDCs (Figures 2C and 2D). Furthermore, the MS sequencing result showed that more pp65 peptides were detected by the moDCs transfected with circular pp65-mRNAs compared with linear pp65-mRNAs at 48 h post-transfection (Figures S2C and S2D), indicating that more pp65 proteins were translated in moDCs transfected with circular pp65-mRNAs.

As shown in Figure 2E, pp65-$Tetramer^+$/$CD8^+$ T cells were expanded from all three individuals carrying HLA-A*02:01, HLA-A*11:01, or HLA-A*24:02 alleles, after two rounds of stimulation with autologous moDCs transfected with both linear or circular pp65 mRNAs. MoDCs transfected with circular pp65 mRNA stimulated a 3- to 6-fold increase in the percentages of $CD8^+$/$Tetramer^+$ T cells compared with linear pp65 mRNA (Figures 2F and 2G). $CD8^+$/$Tetramer^+$ T cells were then subjected to fluorescence-activated cell sorting (FACS) and single-cell TCR sequencing. Interestingly, we found that dominant T cell clones (percentage of 99.64%, 80.96%, and 74.17%, respectively) were selectively expanded from the healthy donors carrying the HLA-A*02:01/HLA-A*11:01/HLA-A*24:02 alleles (Figures 2H and S2E–S2G). These results suggest that cmRNA-transducing moDCs induce a robust expansion of antigen-specific T cells and cmRNA technology therefore constitutes an better tool for *in vitro* priming and expansion of human antigen-specific T cells.

Validation of the activation and killing function of pp65-TCR obtained by cmRNA screening

We subcloned HLA-A*02:01, HLA-A*11:01, and HLA-A*24:02-restricted pp65-responsive TCRs into lentiviral vectors for functional validations. The TCR DNA sequence was codon optimized for efficient TCR expression. To prevent mismatch with the endogenous TCR chain and improve its stability, the constant domains of TCR-α and -β chains were replaced by mouse TRAC and TRBC1, in addition to the complementary cysteine residues at positions 48 (replacing Thr with Cys) and 57 (replacing Ser with Cys) of the constant domains of the TCR-α and -β chains, respectively (Figure 3A). Sequencing revealed two TCR-α genes expressed in the dominant HLA-A*02:01-restricted pp65-responsive T cell clone, and a follow-up *in vitro* binding experiments showed that only one TCR-α gene (TRA:CAFPYNNNDMRF) was responsible for pp65-MHC binding (Figure 3B). As shown in Figure 3C, Jurkat 76 cells or primary $CD8^+$ T cells infected with responsive pp65-TCR lentiviral were stained by pp65-HLA*A:02:01 tetramer. K562 cell lines simultaneously expressing HLA-A*02:01 and pp65 genes (hereafter K562 target cells) were constructed and used as target cells to functionally validate pp65-responsive TCR-T cells. The FACS results showed that lenti-pp65-TCR-T cells were specifically activated by K562 target cells *in vitro*, as evidenced by the observation that the expression of activation markers (CD69 and CD137) and cytokines (interferon [IFN]-γ, tumor necrosis factor [TNF]-α, and granzyme B [GZMB]) were significantly up-regulated in lenti-pp65-TCR-T cells after a 24 h of incubation with K562 target cells (Figures 3D and 3E). The results of the IFN-γ-ELISpot consistently showed a significant increase in the secretion of IFN-γ from lenti-pp65-TCR-T cells after being robustly activated by the K562 target cells, but not by the control HLA-A*02:01-expressing K562 cells lacking pp65 expression (Figures 3F and 3G). To further validate the function of pp65-specific TCRs, pp65-TCR-expressing Jurkat T-NFAT-luciferase reporter cells were co-cultured with target or control cells, and luciferase activities were monitored (Figure 3H). As shown in Figure 3I, pp65-TCR-expressing Jurkat T NFAT-luciferase cells were specifically activated by K562-HLA-A*02:01-pp65 target cells, but not K562-HLA-A*02:01 control cells, *in vitro*.

Next, we tested whether lenti-pp65-TCR-T cells could efficiently kill K562 target cells *in vitro*. We examined the killing efficiency of TCR-T on target cells with different effector:target (E:T) ratios using flow cytometry. As shown in Figure 4A, after a 4-h incubation at an E:T = 10:1, approximately 50% of the K562-HLA-A*02:01-pp65 target cells were killed by TCR-T cells *in vitro*, and about 80% of K562-HLA-A*02:01-pp65 target cells were killed after a 24-h incubation (Figures 4B and 4C). In contrast, less than 20% of K562-HLA-A*02:01 control cells were killed by lenti-pp65-TCR-T cells after 24 h of incubation. In addition, over 30% or 50% of target cells were killed even when an E:T ratio at 1:1, 5:1, or 10:1 was used (Figures 4B and 4C). Meanwhile, we compared the killing efficiency of $CD8^+$ T and pp65-TCR-T cells on target cells using a real-time

Figure 2. Screening procedure for circular pp65 mRNA-mediated pp65 antigen-specific TCR-T

(A) Schematic diagram of *in vitro* screening of CMV-pp65-TCR-T using circular pp65-mRNA. (B) The quantity of linear or circular pp65 mRNA was determined by RT-qPCR at 4, 8, 16, 24, 36, 48, 72, and 96 h after electroporation. (n = 3) (C) pp65 expression at days 1, 2, 5, and 7 after DC electroporation of linear or circular pp65 mRNA by western blot detection. (D) The pp65 expression levels relatives to GAPDH were counted for the linear pp65 mRNA and circular pp65 mRNA groups. (E) The *in vitro* stimulation effect of circular pp65 mRNA was compared with linear mRNA by detecting $CD8^+$/$Tetramer^+$ (%). Flow cytometry was performed to detect the percentage (F) and fold-change (G) of $CD8^+$/$Tetramer^+$ in the linear mRNA group vs. the cmRNA group (n = 3). (H) The frequency of T cell clonotypes was ranked after single cell TCR sequencing. All data represent the mean ± SEM. *$p < 0.05$, ** $p < 0.01$, ****$p < 0.0001$. ns, not significant.

Please cite this article in press as: Shen et al., Circular mRNA-based TCR-T offers a safe and effective therapeutic strategy for treatment of cytomegalovirus infection, Molecular Therapy (2023), https://doi.org/10.1016/j.ymthe.2023.11.017

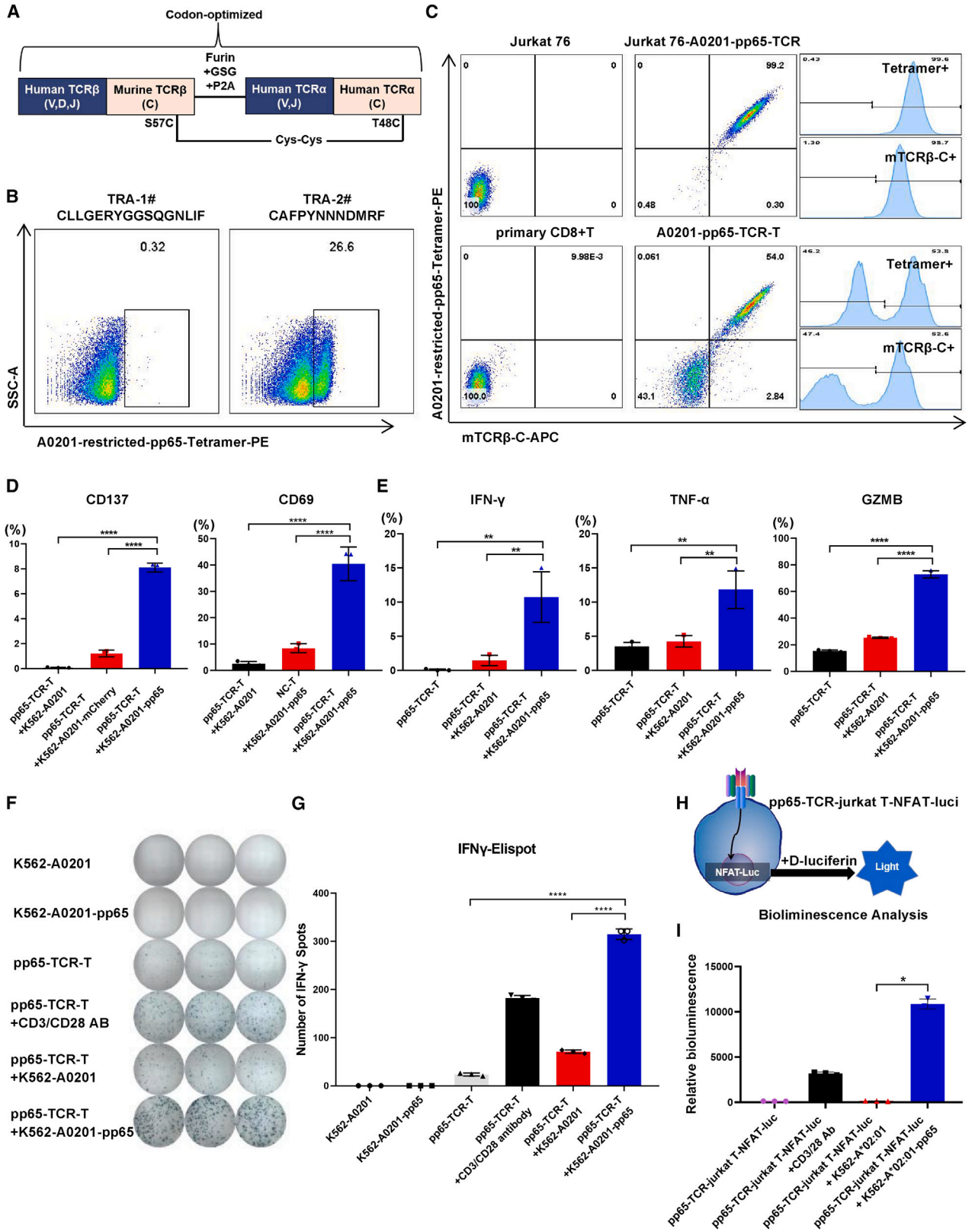

(legend on next page)

live cell imaging analyzer. After 24 h of co-culture at a 5:1 ratio of E:T, about 85% of target cells were killed by pp65-TCR-T cells, significantly higher than that lysed by control $CD8^+$ T cells (Figures 4D and 4E). The results showed that pp65-TCR-T cells were more effective in killing K562-HLA-A*02:01-pp65 target cells than $CD8^+$ T cells *in vitro*.

Then, we aimed to determine the killing efficacy of lenti-pp65-TCR-T cells *in vivo*. The *in vivo* CDX experimental process is illustrated in Figure 4F. A total of 1×10^6 luciferase-labelled K562-HLA-A*02:01-pp65 cells were transplanted into immunodeficient NOD.Cg-Prkdc^{scid}IL2rg^{tm1Sug}/JicCrl (NOG) mice at day 0, and 1×10^7 lenti-pp65-TCR-T cells or mock T cells were transplanted at day 3. Bioluminescence imaging was detected and quantified between 4 and 11 weeks after tumor cell injection. As shown in Figures 4G and 4I, the target cells were efficiently killed in NOG mice transplanted with lenti-pp65-TCR-T cells and all mice survived up to 100 days after target cell transplantation. In contrast, NOG mice that transplanted with mock T cells or saline were unable to eliminate the target cells and all mice died within 11 weeks following target cells transplantation (Figure 4J). Compared with the NOG mice transplanted with mock T cells or saline, the bioluminescence signals appeared to be substantially lowered in NOG mice transplanted with pp65-TCR-T cells (Figures 4G and 4I), which is consistent with the efficient killing activity and long-lasting protection of pp65-TCR-T cells. The results of CDX experiments showed that the lenti-pp65-TCR-T cells could efficiently and specifically kill K562-HLA-A*02:01-pp65-luciferase target cells *in vivo*. The above results collectively showed that the pp65-specific TCR identified by moDCs transfected with circular pp65 mRNAs could specifically bind to the pp65 antigen and T cells transfected with the TCR could effectively recognize and kill target cells both *in vitro* and *in vivo*. We also obtained HLA-A*11:01- and HLA-A*24:02-restricted pp65-TCRs by moDCs transfected with circular pp65 mRNA. The functions of these TCRs were validated by using tetramer staining (Figures S3A and S3B), cytokine release and *in vitro* activation assays (Figures S3C–S3F), and *in vitro* killing assays (Figures S3G and S3H). All of the results further suggested that functional antigen-specific TCRs were obtained using cmRNA technology.

Non-viral, cmRNA delivery system for pp65-TCR transduction

Lentiviral and retroviral vectors have traditionally been used for CAR-T or TCR-T therapies, and CRISPR-based techniques have recently been successfully in integrating CARs into the T cells in a site-specific manner. However, both viral and CRISPR-based methods lead to the integration of CARs or TCRs into the T cell genome, and the long-term safety of these approaches requires careful evaluation. Given our previous results demonstrating strong and sustained protein expressions achieved through cmRNA, we opted to generate non-viral, integration-free TCR-T cells using a cmRNA-based approach and systematically validate their functions *in vitro* and *in vivo*. To this end, we produced cmRNA encoding HLA-A*02:01-restricted, pp65-specific TCR with high purity (98.2%) and a high circulation rate (96.6%) (Figures 5A–5C). Next, primary $CD8^+$ T cells from of HLA-A*02:01-positive donors were expanded *in vitro* for 12 days and then subjected to electrotransfer pp65-TCR cmRNA. As presented in Figure 5D, flow cytometric analysis of the mTCRβ constant region domain revealed more than 90% expression of exogenous TCRs in $CD8^+$ T cells 24 h after electroporation, and T cells can be expanded efficiently *in vitro* after electroporation (Figure S4A).

We next examined the duration of mRNA and protein expression in linear or circular pp65-TCR-mRNA-transduced TCR-T cells by qPCR and flow cytometry. The qPCR results showed that the degradation rate of circular pp65-TCR-mRNA was lower than that of linear mRNA at the same dose of transduction (Figure S4B). Moreover, linear pp65-TCR-mRNA-transduced TCR-T remain a high TCR expression for 72 h and decline rapidly during days 4–7. In contrast, approximately 80% circular pp65-TCR-mRNA-transduced TCR-T cells expressed exogenous TCRs at day7 (Figure 5E). Although the percentages and total fluorescence intensity of exogenous TCR-positive $CD8^+$ T cells eventually declined overtime (Figures 5E and S4C), the total number of $mTCR\beta^+/CD8^+$ T cells remained unchanged, even 10 days after electroporation (Figure 5F), suggesting that the transfected TCR-encoding cmRNA was extremely stable. Moreover, the decreased percentage of exogenous TCR-positive $CD8^+$ T cells could be caused in part by constant T cells divisions overtime.

We then examined the functionality of the primary $CD8^+$ T cells that were electroporated with cmRNA encoding pp65-specific, HLA-A*02:01-restricted TCRs. Our findings showed that cm-pp65-TCR-T cells were specifically activated by K562-HLA-A*02:01-pp65 target cells and not by K562-HLA-A*02:01 control cells. This was indicated by a significant increase in the release of cytokines (IFN-γ and TNF-α) and up-regulation of the activation marker (CD107a) (Figures 5G and 5H). Subsequently, we detected the viability of T cells and the expression of pp65-TCR in T cells 24 h after cmRNA electroporation. As shown in Figure 5I, the viability of T cells dropped from 90% to 70% when 30, 60, 90, 120, and 200 μg of cmRNA were electroporated, and over 95% of surviving T cells expressed pp65-TCR in all groups. We further evaluated the *in vitro* killing efficiency of the cm-pp65-TCR-T cells 1 day after electroporation, using different amounts of

Figure 3. Identification of the function of HLA-A*02:01-restricted pp65-TCR obtained by cmRNA screening

(A) Schematic diagram of CMV-pp65-TCR vector design. (B) *In vitro* Tetramer binding assay was used to verify the correct pp65-TCR sequence. (C–E) *In vitro* binding assay validation using HLA-A*02:01 tetramer after pp65-TCR lentiviral infection of Jurkat 76-CD8 cells and primary $CD8^+$ T cells. Flow cytometry was performed to detect the expression levels of (D) activation-related markers (CD69 and CD137) as well as (E) cytokines (IFN-γ, TNF-α, and GZMB) after co-culturing TCR-T cells with control cells or target cells. (F and G) ELISpot assay was used to detect IFN-γ secretion after co-culture of TCR-T cells with control cells or target cells. (H) Schematic diagram of Jurkat T-NFAT-Luciferase reporter cells. (I) The Jurkat T-NFAT-Luciferase reporter system detects the level of TCR-T activation after co-culture with control or target cells. All data represent the mean ± SEM, n = 3. *p < 0.05, **p < 0.01, ****p < 0.0001.

Please cite this article in press as: Shen et al., Circular mRNA-based TCR-T offers a safe and effective therapeutic strategy for treatment of cytomegalovirus infection, Molecular Therapy (2023), https://doi.org/10.1016/j.ymthe.2023.11.017

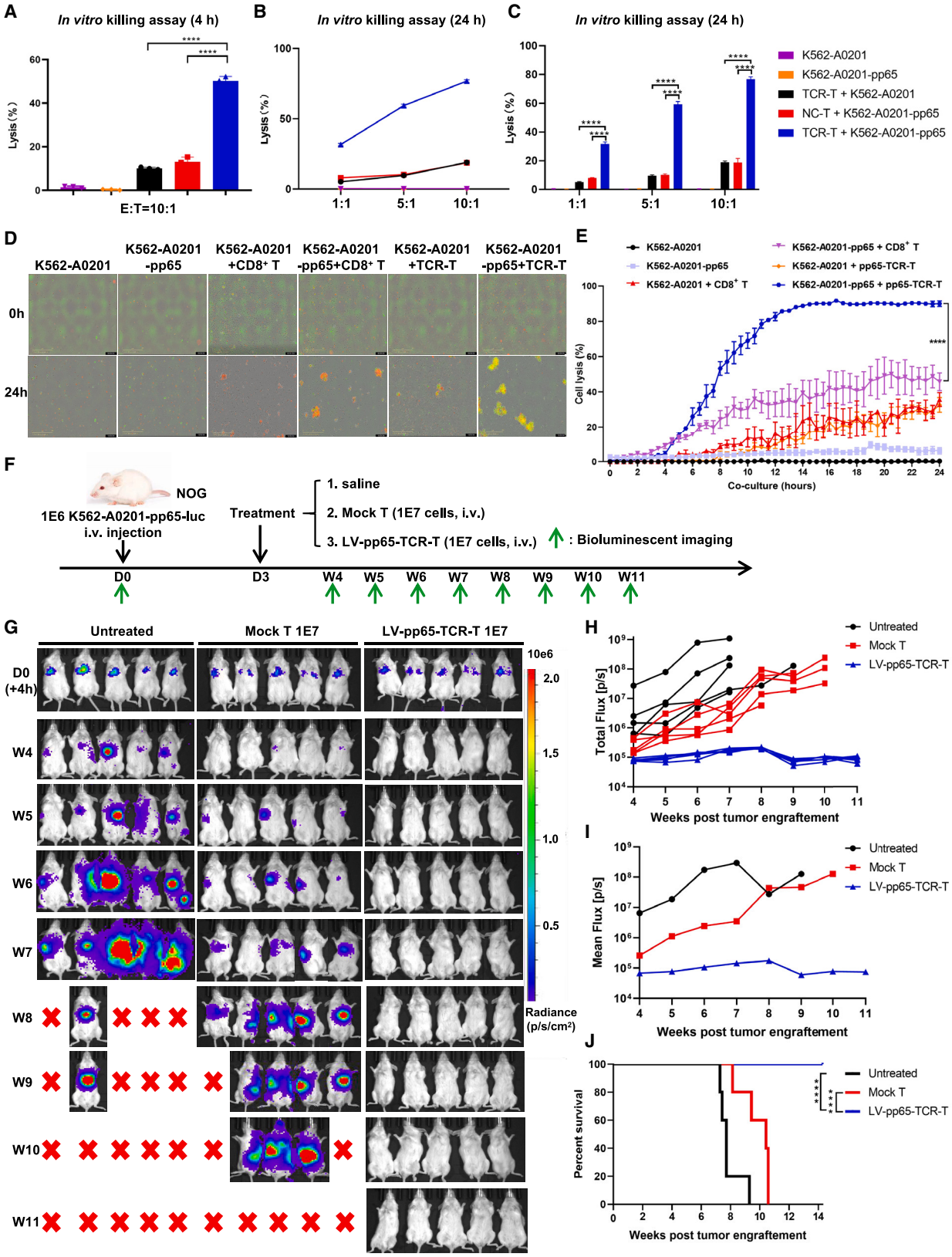

(legend on next page)

electroporated cmRNA and varying E:T ratios. The results, as shown in Figure 5J, demonstrated that cm-pp65-TCR-T cells, electroporated with 120 μg cmRNA, exhibited the highest cytotoxicity at different E:T ratios (1:1, 5:1, and 20:1). Similar results were obtained when the cm-pp65-TCR-T cells, 7 days after electroporation, were used (Figure S4D). These findings indicate that cm-pp65-TCR-T cells can specifically recognize and effectively kill target cells *in vitro*.

Cm-pp65-TCR-T specifically kills the target cells expressing pp65 antigen in an *in vivo* CDX model

We next assessed the feasibility and efficacy of linear or circular pp65-TCR-mRNA-transduced TCR-T cells by an *in vivo* CDX model. As illustrated by Figure 6A, 3×10^6 luciferase-labeled K562-HLA-A*02:01-pp65 cells were transplanted into immunodeficient NOG mice at day 0, and 1×10^7 Mock T or linear mRNA-pp65-TCR-T or cm-pp65-TCR-T cells were injected at day 3, bioluminescence imaging was performed for detection and quantification at weeks 1–5 after tumor cell inoculation. As shown in Figures 6B–6D, all mice injected with saline or mock T cells died within 6 weeks after inoculation with tumor cells. Two mice infused with linear mRNA-pp65-TCR-T cells died at week 5 and one additional mice died at week 6 due to tumor growth (3/6). In contrast, only one mouse died at week 5 in the group of mice infused with cm-pp65-TCR-T cells (1/6) (Figures 6B–6D).

Subsequently, we proceeded to explore whether higher doses and repeat infusions of cm-pp65-TCR-T cells provide prolonged protection. Briefly, 3×10^6 K562-HLA-A*02:01-pp65-luciferase cells were transplanted into immunodeficient NOG mice at day 0, and 2×10^7 mock T cells or cm-pp65-TCR-T cells were infused at day 3 and every 4 days or every 2 weeks thereafter. Bioluminescence imaging was detected and quantified at 1–5 weeks after tumor cell inoculation (Figure 6E). As shown in Figure 6F, all mice infused with either saline or mock T cells died within 40 days after target cells inoculation. In contrast, the mice infused with 2×10^7 cm-pp65-TCR-T cells every 2 weeks survived up to 6 weeks after inoculation of the target cells (Figure 6F). Similar results were observed in the group of mice infused with 2×10^7 cm-pp65-TCR-T cells every 4 days, although there was one mouse died at week 5 for uncharacterized reason. The bioluminescence imaging analysis revealed that the tumor burden of mice infused with cm-pp65-TCR-T cells every 2 weeks or every 4 days were significantly lower than those of the mock T cells (Figures 6G and 6H), and significant body weight loss was observed in the control groups due to the severe tumor burden, whereas a relatively stable body weight was observed in the groups infused with cm-pp65-TCR-T cells (Figure 6I). Moreover, infusions either every 4 days or every 2 weeks of cm-pp65-TCR-T cells significantly prolonged the survival time of the mice (Figure 6J). Collectively, the above results proved that cm-pp65-TCR-T cells specifically and efficiently killed K562-HLA-A*02:01-pp65 cells *in vivo* and provided long-lasting protection for mice against pp65-expressing tumors.

DISCUSSION

The discovery of antigen-specific TCRs is an essential but challenging step for TCR-T cell therapy. This study demonstrated that moDCs transfected with antigen-encoding cmRNA efficiently prime and expand antigen-specific T cells compared with those transfected with linear mRNA. Multiple HLA-A-restricted TCRs targeting CMV pp65 antigen were identified and validated. Moreover, primary $CD8^+$ T cells electroporated with cmRNA encoding pp65-specific TCR genes specifically recognized and efficiently killed target cells *in vitro*, and provided long-lasting protection against pp65-expressing tumor cells *in vivo*. To our knowledge, this study is the first to utilize cmRNAs-based technology to discover antigen-specific TCRs and produce TCR-T cells with therapeutic potential. Although CMV pp65-responsive TCR-T cells were used as a model in this study, we anticipate that the identification of TCRs against other types of antigens, including tumor neoantigens or immunogenic self-antigens, as well as the production of the corresponding TCR-T cells, could readily be obtained by using the cmRNA-based approaches.

Recent studies on circular RNA vaccines for the prevention of SARS-CoV-2, which encode the spike protein, have demonstrated that such vaccines are more effective in antigen production, expression of neutralizing antibodies, and Th1-type immune response levels.[4] These studies suggest that circular RNA may have the potential to extend antigen expression. Prolonged antigen production and presentation in moDCs may provide persistent signaling to the antigen-responsive T cells for sustained activation and proliferation. Indeed, our results demonstrated that moDCs transfected with antigen-encoding cmRNA were more effective at priming and expanding antigen-specific T cells compared with those transfected with linear mRNA *in vitro*. This new cmRNA-based strategy has great potential for the expansion of antigen-specific T cells, particularly for those at relatively low frequencies, thus significantly improving the efficiency of TCRs discovery. The expressions of exogenous TCRs in the human primary T cells transfected with cmRNA were also determined in the study. Compared with a previous study showing that linear mRNA expressed HBV TCRs for 48–72 h,[21,22] our results showed a much longer time period of TCR expression

Figure 4. Identification of the killing function of pp65-TCR-T *in vitro* and *in vivo*

(A–C) The killing efficiency of pp65-TCR-T were detected by Flow cytometry after co-culture with control or target cells at different E:T ratios for 4 h (A) or 24 h (B–C). (D) $CD8^+$T or pp65-TCR-T cells co-cultured 24 h with control or target cell at an E:T = 5:1 (n = 3). Green fluorescent cells were represented K562-HLA-A*02:01 or K562-HLA-A*02:01-pp65 cells. Yellow fluorescent cells were counted as dead cells. Scale bar, 400 μm. (E) The killing efficiency of pp65-TCR-T were detected by Incucyte analysis system after co-culture with control or target cells at E:T = 5:1 (n = 3), scanning interval every 30 min until the killing efficiency assay was completed after 24 h of co-culture. (F) Schematic diagram of the mouse CDX model and procedure of lenti-pp65-TCR-T or mock $CD8^+$ T cell infusion time and dose. (G–I) Bioluminescence imaging analysis of an *in vivo* CDX model, n = 5 mice per group. The tumor burden was quantified as the total flux (H, each line represents single mouse) or mean flux (I) from luciferase intensity of each mouse by bioluminescence imaging. (J) Survival curve analysis of mice in the different treatment groups. All data represent the mean ± SEM, n = 5. ****$p < 0.0001$.

Please cite this article in press as: Shen et al., Circular mRNA-based TCR-T offers a safe and effective therapeutic strategy for treatment of cytomegalovirus infection, Molecular Therapy (2023), https://doi.org/10.1016/j.ymthe.2023.11.017

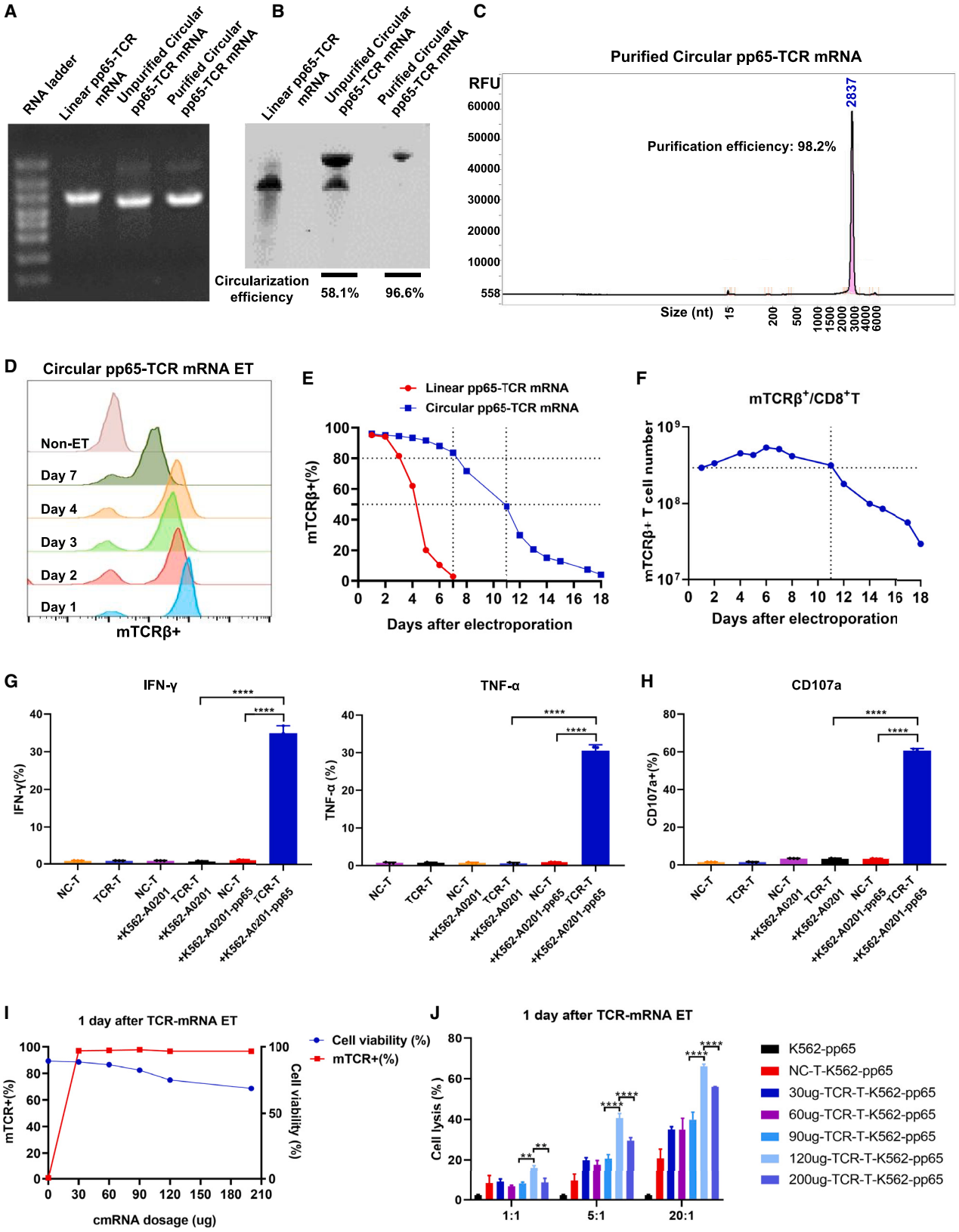

(legend on next page)

by cmRNA, as approximately 80% and 20% of T cells expressed exogenous TCRs 7 or 14 days post-electroporation, respectively. Thus, cmRNA has a higher therapeutic potency than linear mRNA in TCR-T cell-based therapy for viral infections.

CMV infection is a significant cause of morbidity and mortality in patients who undergo allo-HSCT.[20] Our hospital conducted a comprehensive analysis of patients who underwent allo-HSCT between 2018 and 2021, which revealed that 53.5% of patients had experienced a CMV infection at a median time of 56.1 days after HSCT (Figure S2A). Analysis of the patients' postoperative survival revealed that patients who developed CMV infection had a mortality rate of 25.7% at 48 months, which was significantly higher than that of CMV-negative patients ($p < 0.05$) (Figure S2B). Donor-derived CMV-specific cytotoxic T lymphocytes (CMV-CTLs) were used to treat CMV infections after transplantation.[23] However, obtaining donor-derived CMV-CTLs can be difficult for patients whose donors are CMV negative or who have received cord blood or unrelated donor transplants. A recent study has demonstrated the feasibility and efficacy of lentiviral-based TCR-T therapy for treating CMV infections in patients after allo-HSCT, with all patients achieving complete CMV clearance.[24] Nevertheless, lentiviral cause random and permanent integrations in the host genome, and the safety concerns of lentiviral-based vectors are still a matter of debate. CRISPR-based, non-viral adoptive CAR-T or TCR-T cell therapies have recently reported in the treatment of B-NHL and solid tumors.[19,25] However, the aneuploidy and chromosomal truncations caused by CRISPR should be comprehensively evaluated in long-term clinical trials.[26] In this study, we found that infusing cm-pp65-TCR-T cells every 2 weeks effectively eliminated pp65-expressing tumor cells in the CDX mouse models. In clinical practice, most CMV infections occur within 3 months of HSCT, with a low probability of CMV infection once the patients' own anti-CMV immunity is re-established.[27] Therefore, the infusion of cm-pp65-TCR-T cells is only necessary during the first few months after HSCT. Even though cm-pp65-TCR-T cells killed CMV-infected cells in the first couple of weeks after infusion, they lose TCRs eventually, thus representing a safe therapeutic option, especially for patients who have unsatisfactory outcomes following conventional antiviral treatments. The feasibility and efficacy of cm-pp65-TCR-T cell therapy should be assessed in future clinical trials.

The current manufacturing process for CAR-T or TCR-T cells remains highly personalized and time consuming, taking several weeks to produce a sufficient amount of CAR-T or TCR-T cells *in vitro* before infusion back into the patients.[28] *In vivo* CAR-T or TCR-T strategies would overcome these challenges and achieve real off-the-shelf therapies.[29,30] Recent reports have shown that repeated infusions of lipid nanoparticles loaded with linear CAR- or TCR-encoding mRNAs and decorated with targeting antibodies against human T cell surface molecules were able to reduce cancer growth or cardiac fibrosis in mice.[21,30,31] The high stability of cmRNAs in primary human T cells makes cmRNAs an ideal platform for future *in vivo* CAR-T or TCR-T therapies.

Collectively, our findings demonstrate that cmRNAs offer an effective tool for screening of antigen-specific TCRs and a feasible and efficacious non-viral, non-integrating cm-pp65-TCR-T therapy, thus providing a new treatment option for CMV infection following HSCT. With their high safety, exceptional stability, and ease of manufacturing, cmRNA platforms hold promise as a therapeutic option for a wide range of diseases.

MATERIALS AND METHODS

Cell lines, primary cells, and animals

K562 and HEK293T cell lines were purchased from the ATCC and the Jurkat T NFAT-luciferase reporter cell line was purchased from ACRO biosystems company (CJUR-STF046#). HEK293T cells were maintained in DMEM mediums (Gibco) supplemented with 10% (v/v) fetal bovine serum (FBS, Gibco). K562 and Jurkat T cells were maintained in RPMI-1640 mediums (Gibco) supplemented with 10% (v/v) FBS. Human primary monocytes and T cells were cultured in complete RPMI-1640 medium supplemented with 10% human serum (GeminiBio). Cells were cultured in a 37°C incubator under 5% (v/v) CO_2. NOG mice (female, 4–6 weeks old) were purchased from Charles River Laboratories. All the mice were maintained under specific pathogen free conditions. Animal studies were approved by the Institutional Animal Care and Use Committee (IACUC, 2021AW041), Shanghai General Hospital. The collection criteria for blood specimens involving healthy donors were approved by the Ethics Committee of Shanghai General Hospital (EC, 20230113032724383).

PBMCs collection and HLA typing

Healthy donors (HDs) signed informed consent before donating granulocyte colony stimulating factor mobilized peripheral blood stem cells (PBMCs), and PBMCs were again isolated by density-gradient

Figure 5. Functional characterization of cm-pp65-TCR-T *in vitro*

(A and B) Agarose gel electrophoresis (A) and urea PAGE (B) experiments were performed to analyze the circularization efficiency of PIE of pp65-TCR cmRNA. (C) Capillary electrophoresis experiments were used to analyze the percentage of pp65-TCR cmRNA, and the purification efficiency values are marked in the figure. (D) Ridge plot showing the change of mTCRβ$^+$% of T cells electrotransfered pp65-TCR cmRNA within 7 days. (E) Plot of mTCRβ$^+$% within 18 days after T cell electrotransfer of linear or circular pp65-TCR mRNA. X axis dashed line indicates day 7 or day 11, Y axis dashed line indicates mTCRβ$^+$ at 80% or 50%. (F) Total fluorescence intensity of all cells within 18 days after T cell electrotransfer of pp65-TCR cmRNA. The dashed line on the X axis indicates day 11, and the dashed line on the Y axis indicates the number of cells on the first day after electrotransfer. (G and H) Flow cytometry was performed to detect the expression levels of cytokines (IFN-γ and TNF-α), as well as activation-related markers (CD107a) after co-culture of cm-pp65-TCR-T cells with control cells or target cells. (I) T cell viability and pp65-TCR expression levels 24 h after electroporation of different doses of pp65-TCR cmRNA (per 1×10^7 T cell) were measured by flow cytometry. (J) After cm-pp65-TCR-T co-culture with control or target cells at different E:T ratios or different doses of cmRNA for 4 h, the killing efficiency was observed for the cm-pp65-TCR-T cells 1 day after electroporation. All data represent the mean ± SEM, n = 3. $^{**}p < 0.01$, $^{****}p < 0.0001$.

Please cite this article in press as: Shen et al., Circular mRNA-based TCR-T offers a safe and effective therapeutic strategy for treatment of cytomegalovirus infection, Molecular Therapy (2023), https://doi.org/10.1016/j.ymthe.2023.11.017

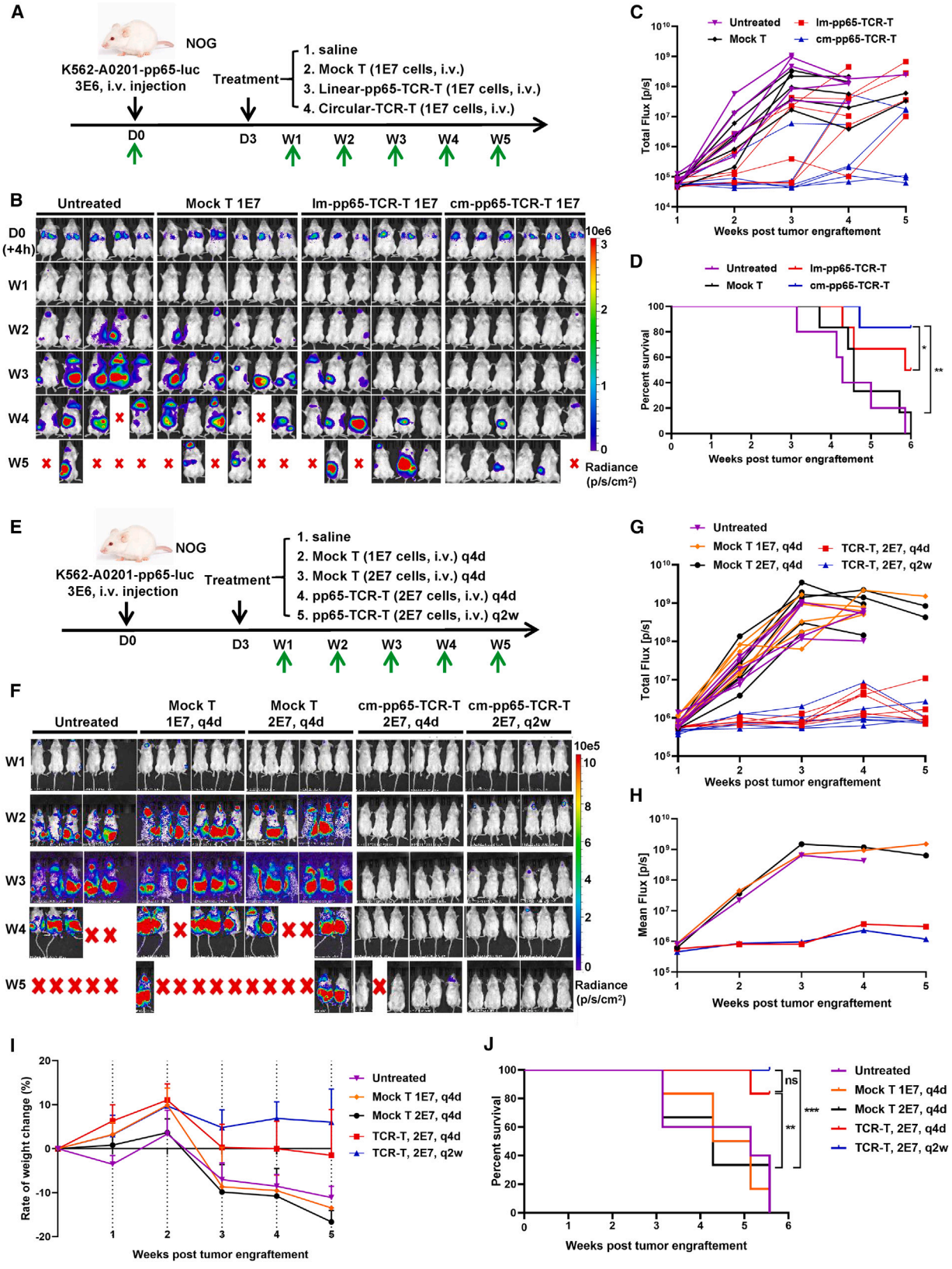

(legend on next page)

centrifugation using lymphocyte separation medium (Corning) and cryopreserved until ready for use. High-resolution genomic HLA typing for HDs was performed by Tissuebank Biotechnology.

Plasmids and lentiviral transduction

pCDH-CMV-MCS-Puro, pCDH-CMV-pp65-TCR-Puro, pMDLg/pRRE, pRSV-Rev, and pMD2.G plasmids were purchased or synthesized from Youbio Biotechnology. pSFFV-CMV-pp65-mCherry-IRES-luciferase and pSFFV-HLA-A*02:01-GFP plasmids were synthesized by Biovision Biotechnology. HEK293T cells were transfected with pCDH-CMV-pp65-TCR-Puro plasmid and viral packaging plasmids pMDLg/pRRE, pRSV-Rev, and pMD2.G using Opti-MEM reagent (Gibco). At 48 h post-transfection, lentiviral supernatants were collected, filtered through 0.45-microporous membrane filters, concentrated by ultracentrifugation and frozen in aliquots at −80°C prior to use.

In vitro stimulation of antigen-specific TCR-T

PBMCs of healthy HLA-A*02:01/HLA-A*11:01/HLA-A*24:02 donors were seeded in six-well plates at 2×10^7 cells/well in complete medium for 90 min at 37°C in the absence of cytokines to separate adherent (containing monocytes) and non-adherent cells (containing T cells). $CD8^+$ T cells were enriched from non-adherent fractions by positive selection kit (STEMCELL Technologies). To generate immature moDCs, adherent fractions were washed with PBS followed by fresh complete 1640 medium supplemented with recombinant human IL-4 (50 ng/mL, PeproTech) and granulocyte macrophage colony stimulating factor (GM-CSF) (100 ng/mL, PeproTech). Fresh IL-4 and GM-CSF were supplemented every 2 days for induction for 5 days, and moDCs were stimulated with 10 ng/mL IL-1β, TNF-α, IL-6, and PGE2 (PeproTech) for 24 h before transfection to induce moDCs maturation. CMV-pp65 linear or cmRNA at a concentration of 100 μg/mL was electrotransfected into moDCs using the Gene Pulser X cell system (Bio-Rad). After electrotransfection, HD T cells were co-cultured with pp65-loaded mature moDCs at an E:T ratio of 2.5:1 in the presence of IL-21 (30 ng/mL, PeproTech) in 24-well plates. During *in vitro* culture, supplement the wells with fresh medium containing IL-2, IL-7, and IL-15 (5 ng/mL each) every 3 days.

Flow cytometry

For extracellular staining, after collection, cells were washed twice with staining buffer (DPBS supplemented with 2% FBS) and stained with eBioscience Viability Dye eFluor780 (Thermo Fisher Scientific) for 20 min at room temperature (RT). The cells were then washed with staining buffer, treated with Fc-Block (BD Biosciences) for 10 min at RT and then stained with the cell surface antibodies for 30 min at RT, then washed with staining buffer, resuspended with 500 μL staining buffer and collected on LSRFortessa (BD Biosciences). For intracellular staining, after extracellular staining, cells are washed with staining buffer and then fixed and permeabilized with the BD Cell Fixation/Permeabilization solution kit according to the manufacturer's instructions (BD Biosciences). Cells were washed with perm/wash solution, followed by intracellular staining with intracellular antibody (30 min at RT). Finally, cells were washed and resuspended with 500 μL of perm/wash buffer. Samples were washed and collected on LSRFortessa (BD Biosciences). Analysis was performed using FlowJo software. Flow cytometry antibodies used in this study for both intracellular and extracellular staining are listed in Table S1.

Trypsin digestion and MS

Cells were harvested and washed three times with PBS. They were then gently pipetted up and down for overnight in 1 mg/mL trypsin. The supernatant was then centrifuged at 13,000 rpm for 30 min and frozen at −80°C. The Orbitrap Fusion (Thermo Fisher Scientific) was coupled online to an ultra-high-performance LC (1290 Infinity, Agilent) via a nanoelectrospray ion source (Nanospray Flex, Thermo Fisher Scientific). Samples were loaded at a flow rate of 5 μL/min for 5 min onto a 2 cm × 100 μm C18 trapping column packed in-house with C18 beads of 3 μm diameter (ReproSil-Pur C18-AQ, Dr. Maisch GmbH). Peptides were then separated on a 50 cm × 75 μm column in-house filled with C18 beads of 2.7 μm diameter (Poroshell 120 EC-C18, Agilent). Separation was run at 21°C using a flow rate of approximately 300 nL/min and a 90-min gradient ranging from 5.6% CH_3CN to 32% CH_3CN in 0.1% HCOOH. MS1 scans were acquired at a resolution of 60,000 at 200 Th.

Tetramer labeling assay

HLA-A*02:01/HLA-A*11:01/HLA-A*24:02 tetramers bound to CMV-pp65 NV9/AK9/QF9 and conjugated to PE were purchased from MBL Biotechnology. Cells were labeled with PE-conjugated tetramer for 15 min at RT, followed by surface antibodies against CD3, CD8, and live/dead dye for an additional 20 min at 4°C. After staining, cells were washed 3 times with FACS buffer (DPBS supplemented with 2% FBS) and detected on a BD LSRFortessa flow cytometer, or cells were sorted on BD ARIES III flow cytometer.

Figure 6. Validation of the killing function of cm-pp65-TCR-T by CDX model

(A) Illustration for the evaluation of the *in vivo* killing efficacy of targeting CMV-pp65-expressing tumor cells using linear mRNA-pp65-TCR-T or cm-pp65-TCR-T. (B) Bioluminescence imaging analysis of an *in vivo* CDX model, and the tumor burden was quantified as the total flux (C). (D) Survival curves were analyzed for mice in the untreated group (n = 5) or different cell treatment groups (n = 6). (E) Experimental overview for the evaluation of the *in vivo* killing efficacy and safety of targeting CMV-pp65 using cm-pp65-TCR-T or mock $CD8^+$ T cells. (F and H) Bioluminescence imaging analysis of an *in vivo* CDX model. The tumor burden was quantified as the total flux (G) and mean flux (H) (untreated group, n = 5; cell treatment group, n = 6). (I) Weight monitoring was performed once a week following tumor cell injection. (J) Survival curve analysis of mice in different treatment groups. All data represent the mean ± SEM. ns, no significant difference. *$p < 0.05$, **$p < 0.01$, ***$p < 0.001$. Zhang and colleagues reported that TCR-T represent a promising means of treating viral infections. Circular-mRNA can be used for TCR isolation and identification. Cm-pp65-TCR-T cells provide a safe, non-viral, non-integrated therapeutic approach for controlling CMV infection, particularly in patients who have undergone allogeneic hematopoietic-stem-cell-transplantation.

Single-cell immune profiling

FACS-sorted $CD8^+$/$Tetramer^+$ cells were harvested, final cell concentration was determined by cell count on a hemocytometer, and the cell concentration was adjusted to approximately 1,000 cells/μL with a cell viability of greater than 98%. We prepared sorted $CD8^+$/$Tetramer^+$ T cells for 10× Genomics single-cell sequencing of rearranged VDJ according to manufacturer's instructions. Detailed quality control metrics were generated and evaluated using single-cell analysis packages from Bioconductor, including DropletUtils, scater, and scran. Genes detected in fewer than 3 cells and cells where fewer than 200 genes had non-zero counts were filtered out and excluded from subsequent analysis. Low-quality cells with more than 15% of the read counts derived from the mitochondrial genome were also discarded. After single-cell sequencing and analysis, the TCR sequences were evaluated using the Loupe VDJ browser (Cell Ranger, 10× Genomics), and the top ten rankings were performed according to the frequency of TCRs, and the first-ranked human TCRα and TCRβ chain sequences were selected for subsequent functional experiments.

Human T cell culture and lentiviral transduction

Human $CD8^+$ T cells were isolated from PBMCs of HDs with EasySeq Human CD8 Pos. Sel. Kit II (STEMCELL Technologies). $CD8^+$ T cells were cultured in RPMI-1640 medium supplemented with 10% FBS and 50 U/mL hIL-2 (PeproTech). $CD8^+$ T cells were stimulated with Dynabeads Human T-Expander CD3/CD28 (Thermo Fisher Scientific) at a bead-to-cell ratio of 2.5:1 for 48 h before lentiviral infection. Resuspend 3×10^6 T cells in 2 mL lentiviral supernatant containing 50 U/mL IL-2 and 5 μg/mL protamine sulfate. Plate into wells of six-well plates. Spinfect by centrifuging cells 90 min at $800\times g$ at 30°C, and then incubate overnight at 37°C in a 5% CO_2 cell culture chamber. Discard the supernatant after centrifugation, resuspend with 1640 medium containing IL-2 (50 U/mL) to a final volume of 4 mL/well. Infection efficiency was detected by flow cytometry at days 2 after two rounds of lentiviral infection.

Vector construction and mRNA preparations

DNA synthesis and gene cloning were customized and performed by Genewitz. Linear mRNA were synthesized by *in vitro* transcription from linearized plasmids using the Purescribe T7 High Yield RNA Synthesis Kit (CureMed Biotech). For the generation of cmRNA, DNA fragments containing PIE elements, Internal Ribosome Entry Sites, coding regions, and other elements were chemically synthesized and cloned into a linearized pUC57 plasmid digested with a restriction enzyme. cmRNA precursors were synthesized by *in vitro* transcription from a linearized plasmid using a Purescribe T7 High Yield RNA Synthesis Kit. RNA was then purified, after which guanosine triphosphate was added to a final concentration of 2 mM along with a buffer including magnesium (Thermo Fisher Scientific). cmRNA was analyzed using 1% agarose gel electrophoresis and a ssRNA ladder (Thermo Fisher Scientific) was used as a standard.

cmRNA purification

For high-performance liquid chromatography, RNA was loaded onto a 30- to 300-mm size exclusion column with a particle size of 5 mm and a pore size of 1,000 Å (Sepax Technologies) on an SCG (Sepure Instruments) protein purification system (Sepure Instruments). Then the column was eluted with RNase-free phosphate buffer (pH = 6.0) and chromatography was performed at a flow rate of 15 mL/min. RNA with high purity was collected by peak capture and concentrated, and the buffer was replaced with RNase-free water following ultra-centrifugation.

Electrotransfer of GFP or pp65-mRNA to moDCs

Human mature moDCs pellets were collected by centrifugation at 1,000 rpm for 5 min, cell culture medium was removed, and moDCs were washed twice with 5 mL 1× PBS, cell pellets were re-suspended in an electroporation buffer Opti-MEM (Thermo Fisher Scientific), and the cell concentration was adjusted to be 1×10^7 cells/mL. We mixed 2 μg linear mRNA (approximately 367 nM) or circular GFP mRNA (approximately 190 nM) carefully with the cell suspension prior to transfection. We mixed 100 μL cell suspension with GFP mRNA and transferred it into a 2-mm electroporation cuvette (Bio-Rad), and electroporation was performed using Gene Pulser Xcell system (Bio-Rad). GFP expression was evaluated by fluorescence imaging using a fluorescence microscope (Vert-A1, ZEISS) and flow cytometry analysis (Foretessa, BD). pp65 expression was evaluated by western blot and MS.

RT-qPCR

DC cells were collected at 4, 8, 16, 24, 36, 48, 72, and 96 h after GFP/pp65-mRNA electroporation. $CD8^+$ T cells were collected at 1, 4, 8, 24, 48, and 72 h after pp65-TCR-mRNA electroporation. Total RNA was extracted using the EZ-press RNA purification kit (EZBioscience) according to the protocol. Reverse transcription of 1 mg of total RNA was performed using the PrimeScript RT kit (Takara, Japan), RT-qPCR was then performed using SYBR Green Pre-mix Pro Taq HS qPCR Kit (Accurate). The primers used for RT-qPCR were as follows: GFP-FP:5′-GAAGAACGGCATCAAGGTG-3′; GFP-RP:5′-GGACTGGGTGCTCAGGTAG-3′; pp65-FP: 5′-GGCA AGATCAGCCACATCA-3′; pp65-RP: 5′-TCAGCT- CCACGGT CTCCCT-3′; pp65-TCR-FP: 5′-AAACCCATGGGACGCTCTTA-3′; pp65-TCR-RP: 5′-TGGGATTAGCCGCATTCAGG-3′.

Western blot

Cell lysates were separated by 10% SDS-PAGE and transferred to the polyvinylidene fluoride membrane. The membrane was then blocked with 5% non-fat dry milk (dissolved in TBST buffer) for 1 h, followed by an overnight incubation with GFP mAb (#2956, Cell Signaling Technology) or CMV pp65 mAb (sc-52401, Santa Cruz Biotechnology) or GAPDH mAb (#97166, Cell Signaling Technology). Subsequently, the membranes were washed three times with TBST, the membranes were then incubated with anti-mouse or anti-rabbit IgG, horseradish peroxidase (HRP)-linked Antibody (#7076, #7074, Cell Signaling Technology) at RT for 2 h. Then, the membranes were washed three times with TBST and visualized by Omni-ECL kit (Epizyme, China), imaging was then performed using a biochemi-luminometer (General Electric, AI600). Finally, western blot bands were quantified in grayscale using ImageJ software.

cmRNA-mediated production procedures in cm-pp65-TCR-T cells

Human primary $CD8^+$ T cells were electroporated to express HLA-A*02:01-restricted pp65-TCR (1# clonetype). Cell pellets were collected by centrifugation at 1,000 rpm for 5 min, cell culture medium was removed, and T cells were washed twice with 5 mL 1× PBS, cell pellets were re-suspended in an electroporation buffer Opti-MEM (Thermo Fisher Scientific), and the cell concentration was adjusted to be 1.5×10^8 cells/mL. Note that indicated amount of cmRNA was carefully mixed with the cell suspension prior to transfection. We then transferred 300 μL of cell suspension mixed with cmRNA into an electroporation cup, and electroporation was performed using X-porator H1 (Etta Biotech). Electroporation efficiency was quantified by staining with the antigen-presenting cell-conjugated anti-mouse TCRβ chain antibodies (BioLegend).

TCR sequence optimization and TCR-T cell preparation

After the pp65-TCR sequences were obtained by single-cell sequencing, the sequences were optimized, including (1) Human constant regions of pp65-TCR were replaced by mouse Trbc1 and Trac constant regions, and threonine at positions 48 of Trac and serine at positions 57 of Trbc1 were changed to cystines, these two mutations will enhance the pairing of exogenous TCR while preventing mismatch with endogenous TCR chains; (2) human codon optimization of the expression sequence to improve the expression of TCR protein; and (3) use of P2A and Furin-cleavage to make alpha and beta chains can be expressed simultaneously on one plasmid.

Resuspend PBMCs at 1×10^7 cells/mL in CTL medium. Add Dynabeads Human T-Expander CD3/CD28 (Gibco) at a 3:1 bead/$CD3^+$ T cell ratio. We resuspended in 10 mL CTL medium containing 50 U/mL IL-2 and transferred them into a T25 flask, and then cultured PBMCs for 48 h in a 37°C incubator. We resuspended 5×10^6 T cells in 2 mL lentiviral supernatant containing 100 U/mL IL-2 and 5 μg/mL protamine sulfate; cells were then placed in wells of a 12-well plate and centrifuged at 1,000×*g* for 90 min. We incubate the cells overnight at 37°C, 5% CO_2 after centrifugation, a second round of lentiviral infection was performed 24 h after the first round of infection. We harvested one well of the 12-well plate for flow cytometric analysis of T cell transduction efficiency by staining with peptide:HLA Tetramer or anti-mTCRβC antibody at day5. We removed beads according to the manufacturer's instructions, monitored cells daily, and split them into 6-well plates or T25 flask as necessary for up to 14 days.

In vitro binding assays

Jurkat 76-CD8 T cells or human primary $CD8^+$ T cells from HLA-A*02:01, HLA-A*11:01, or HLA-A*24:02 HDs were infected with CMV-pp65-TCR lentiviral for two rounds, followed by CMV-pp65-HLA-A*02:01, CMV-pp65-HLA-A*11:01, or CMV-pp65-HLA-A*24:02 tetramer staining. The population of $Tetramer^+/mTCR\beta^+$ Jurkat 76 and $Tetramer^+/mTCR\beta^+$ primary $CD8^+$ T cells was then analyzed by flow cytometry.

In vitro activation assays

According to an E:T of 1:1, we inoculated pp65-TCR-T cells with K562-HLA-GFP or K562-HLA-GFP-mCherry or K562-HLA-pp65-mCherry cells in round-bottom 96-well plates. After 24 h of co-culture, extracellular staining was performed, and then the membrane was fixed and ruptured, and after intracellular staining, flow cytometry was used to detect the expression levels of CD25, CD69, CD107a, CD137, TNF-α, GZMB, and IFN-γ in $CD8^+$ T cells in the co-culture system.

For enzyme-linked immunospot (ELISpot) assays, we diluted the coated antibody (1.5 μg/100 μL) with DPBS, added 100 μL of the diluted 1-D1K antibody solution to each well, and incubated it at 4°C overnight (Mabtech, Sweden). We removed the antibody in the plate, wash with sterile DPBS, plated the cells in an E:T ratio of 1:1, added 3×10^4 CMV-pp65-TCR-T cells, K562-HLA-A*02:01, or K562-HLA-A*02:01-pp65 cells to each well, tapped the edge of the plate to spread the cells evenly, and placed them in an incubator at 37°C, 5% CO_2 for 20 h. After 20 h, the cells were removed, washed five times with DPBS to completely remove the cells, and then 100 μL biotin-labeled detection antibody 7-B6-1-biotin was added to each well and incubated at 37°C for 2 h. After the incubation, the plate was washed five times with DPBS, and then 200 μL streptavidin-HRP was added to each well, and incubated at 37°C for 1 h. After the incubation, the plate was washed five times with DPBS, and 100 μL substrate TMB was added to each well until clear spots appeared. Finally, deionized water was added to stop the reaction. Statistical analysis was performed after the ELISpots reader instrument scanned the plates.

For the Jurkat T-NFAT-luciferase reporter system, we counted viable cells and harvested the cells and plated the cells at a density of 5×10^4 cells/well in 96-well culture plates (Round Bottom) in 40 μL 1640 medium. According to an E:T of 1:1, we inoculated pp65-TCR-T cells with K562-HLA-GFP or K562-HLA-pp65-mCherry cells. We added 5 μg/mL anti-human CD3/CD28 antibody in 40 μL of 1640 medium to positive control wells. We incubated them at 37°C with 5% CO_2 for 12 h. We added 80 μL ONE-Glo Luciferase reagent (Promega) per well and rock at RT for 2 min to allow complete cell lysis. We mixed by pipettor action and transfer 110 μL to a corresponding 96-well Bioluminescence detection plate. We read the relative luminescence units of the plate using a luminescence plate reader.

In vitro killing assays

For flow cytometry assay, we gently resuspended the K562 cells in the CellTrace violet dye solution (Thermo Fisher Scientific) and incubated the cells for 20 min at RT or 37°C, protected from light. We pelleted the cells by centrifugation and resuspended them in fresh, prewarmed complete culture medium, inoculated them pp65-TCR-T cells and K562-HLA control cells or K562-HLA-pp65 target cells into round-bottomed 96-well plate at an E:T ratio of 1:1, 5:1, 10:1, or 20:1. After 4 h or 24 h of co-culture, the $CellTrace\ violet^+/eFluor780^+$ (live/dead) ratio of K562-HLA or K562-HLA-pp65 in

the co-culture system was detected by FACS to evaluate the killing efficiency of CMV-pp65-TCR-T cells.

For Incucyte Live Cell Imaging assay, co-cultures of pp65-TCR-T cells or $CD8^+$ T cells with an E:T ratio of 5:1 and K562-A0201 control cells or K562-A0201-pp65 target cells were added to 96-well plates. The Incucyte Annexin V Dyes reagent (Sartorius) can then be diluted in complete medium to a final dilution of 1:200. The 96-well plate containing the cells is placed into the Incucyte Live Cell Assay Instrument (Sartorius) and apoptosis is monitored using the appropriate fluorescent channel. Specific parameters were as follows. The observation magnification was 20× objective, channel selection, Green|Red|Orange; and scanning interval, every 30 min until the killing efficiency assay was completed after 24 h of co-culture. At the end of the assay, the *in vitro* killing efficiency of pp65-TCR-T was analyzed using Incucyte Live Cell Analysis System software.

Cell-derived xenograft and bioluminescence detection

For lentiviral-based TCR-T experiments, 1×10^6 K562-HLA-A*02:01-pp65-luciferase cells were injected into the lateral tail vein of NOG mice at day 0 and 200 μL saline, 1×10^7 Mock $CD8^+$ T cells or LV-pp65-TCR-T cells were injected through the lateral tail vein at day 3.

For linear mRNA or cmRNA-based TCR-T experiments, 3×10^6 K562-HLA-A*02:01-pp65-luciferase cells were injected into the lateral tail vein of NOG mice at day 0; 200 μL saline, 1×10^7 or 2×10^7 Mock $CD8^+$ T cells, linear mRNA-pp65-TCR-T or cm-pp65-TCR-T cells were injected through the lateral tail vein at day 3. The mice in the cm-pp65-TCR-T groups were subdivided into every 4 days, every 2 weeks injection groups. For bioluminescence imaging, 15 min after intraperitoneal injection of 10 μL/g D-luciferin potassium salt (15 mg/mL, Beyotime), the expression of luciferase in tumor cells was detected by bioluminescence imaging of mice, and the total or mean photon number intensity of luciferase were quantified.

Statistical analysis

Results are expressed as mean ± SEM of at least three independent experiments performed in triplicate. Sample sizes for *in vitro* experiments were $n \geq 3$. Sample sizes for *in vivo* experiments were $n \geq 5$. A Gaussian distribution was used to test if the samples are normally distributed. If the samples conformed to normal distribution, experiments comparing two groups were then analyzed by Student's *t*-test. For experiments comparing three or more groups, one-way ANOVA or two-way ANOVA was performed, and groups were post hoc compared using Tukey's multiple comparison test. If the samples do not conform to a normal distribution, a non-parametric test is used and will be compared using the Wilcoxon test. For *in vivo* experiments, survival curve analyses were performed using the log rank Mantle-Cox test. All statistical analyses were performed using GraphPad Prism version 8.0 software. A p value of less than 0.05 was considered a statistically significant difference.

DATA AND CODE AVAILABILITY

The datasets generated during and/or analyzed during the current study are available from the corresponding author on reasonable request.

SUPPLEMENTAL INFORMATION

Supplemental information can be found online at https://doi.org/10.1016/j.ymthe.2023.11.017.

ACKNOWLEDGMENTS

This study was supported by National Key R&D Program of China, China (2021YFC2502300, 2019YFA0111000); Science and Technology Commission of Shanghai Municipality of China, China (19JC1414400); Two-hundred Talent team project from Shanghai Jiao Tong University School of Medicine, China; Three-year development project from Shanghai Shen Kang Hospital Development Center, China (SHDC2020CR1012B); and Clinical research projects of key disciplines in Shanghai General Hospital, China (CCTR-2022ZD07). "Open Competition to Select the Best Candidates" Key Technology Program for Nucleic Acid Drugs of National Center of Technology Innovation for Biopharmaceuticals of China, China (NCTIB2022HS02012). The authors gratefully acknowledge the assistance of the Flow cytometry Core Facility for and Animal Core Facility of Shanghai General Hospital. We thank Mr. Lau Ngai Cheung Patrick for the financial support of this project.

AUTHOR CONTRIBUTIONS

Conception, design, and supervising of the study: Y.Z. and X.S.; development of methodology and acquisition of data: L.S., J.Y., J.X., L.M., P.W., Q.H., X.Z., X.D., L.W., S.J., L.M.; and B.Z.; analysis and interpretation of data: L.S. and J.Y.; technical and material support: C.Z., Z.S., M.Z., and Y.Y.; clinically relevant guidance: X.S., L.W., X.D., and B.D. All authors read and approved the final manuscript.

DECLARATION OF INTERESTS

One patent has been filed to protect cmRNA as well as its application (inventors C.Z. and Z.S.), three patents have been filed to protect HLA-A*02:01/HLA-A*11:01/HLA-A*24:02-restricted pp65-TCR sequence as well as their applications (inventors P.W., L.S., X.S., and Y.Z.).

REFERENCES

1. Polack, F.P., Thomas, S.J., Kitchin, N., Absalon, J., Gurtman, A., Lockhart, S., Perez, J.L., Pérez Marc, G., Moreira, E.D., Zerbini, C., et al. (2020). Safety and Efficacy of the BNT162b2 mRNA Covid-19 Vaccine. N. Engl. J. Med. *383*, 2603–2615.

2. Chakraborty, C., Sharma, A.R., Bhattacharya, M., and Lee, S.S. (2021). From COVID-19 to Cancer mRNA Vaccines: Moving From Bench to Clinic in the Vaccine Landscape. Front. Immunol. *12*, 679344.

3. Wesselhoeft, R.A., Kowalski, P.S., and Anderson, D.G. (2018). Engineering circular RNA for potent and stable translation in eukaryotic cells. Nat. Commun. *9*, 2629.

4. Qu, L., Yi, Z., Shen, Y., Lin, L., Chen, F., Xu, Y., Wu, Z., Tang, H., Zhang, X., Tian, F., et al. (2022). Circular RNA vaccines against SARS-CoV-2 and emerging variants. Cell *185*, 1728–1744.e16.

5. Liu, C.X., and Chen, L.L. (2022). Circular RNAs: Characterization, cellular roles, and applications. Cell *185*, 2390.

6. Wesselhoeft, R.A., Kowalski, P.S., Parker-Hale, F.C., Huang, Y., Bisaria, N., and Anderson, D.G. (2019). RNA Circularization Diminishes Immunogenicity and Can Extend Translation Duration In Vivo. Mol. Cell *74*, 508–520.e4.
7. Puttaraju, M., and Been, M.D. (1992). Group I permuted intron-exon (PIE) sequences self-splice to produce circular exons. Nucleic Acids Res. *20*, 5357–5364.
8. Yang, J., Zhu, J., Sun, J., Chen, Y., Du, Y., Tan, Y., Wu, L., Zhai, M., Wei, L., Li, N., et al. (2022). Intratumoral delivered novel circular mRNA encoding cytokines for immune modulation and cancer therapy. Mol. Ther. Nucleic Acids *30*, 184–197.
9. van de Donk, N.W.C.J., Usmani, S.Z., and Yong, K. (2021). CAR T-cell therapy for multiple myeloma: state of the art and prospects. Lancet Haematol. *8*, e446–e461.
10. Mullard, A. (2021). FDA approves first BCMA-targeted CAR-T cell therapy. Nat. Rev. Drug Discov. *20*, 332.
11. Tawara, I., Kageyama, S., Miyahara, Y., Fujiwara, H., Nishida, T., Akatsuka, Y., Ikeda, H., Tanimoto, K., Terakura, S., Murata, M., et al. (2017). Safety and persistence of WT1-specific T-cell receptor gene-transduced lymphocytes in patients with AML and MDS. Blood *130*, 1985–1994.
12. Shafer, P., Kelly, L.M., and Hoyos, V. (2022). Cancer Therapy With TCR-Engineered T Cells: Current Strategies, Challenges, and Prospects. Front. Immunol. *13*, 835762.
13. Huang, J., Brameshuber, M., Zeng, X., Xie, J., Li, Q.J., Chien, Y.H., Valitutti, S., and Davis, M.M. (2013). A single peptide-major histocompatibility complex ligand triggers digital cytokine secretion in CD4(+) T cells. Immunity *39*, 846–857.
14. Sykulev, Y., Joo, M., Vturina, I., Tsomides, T.J., and Eisen, H.N. (1996). Evidence that a single peptide-MHC complex on a target cell can elicit a cytolytic T cell response. Immunity *4*, 565–571.
15. Parkhurst, M., Gros, A., Pasetto, A., Prickett, T., Crystal, J.S., Robbins, P., and Rosenberg, S.A. (2017). Isolation of T-Cell Receptors Specifically Reactive with Mutated Tumor-Associated Antigens from Tumor-Infiltrating Lymphocytes Based on CD137 Expression. Clin. Cancer Res. *23*, 2491–2505.
16. Ali, M., Foldvari, Z., Giannakopoulou, E., Böschen, M.L., Strønen, E., Yang, W., Toebes, M., Schubert, B., Kohlbacher, O., Schumacher, T.N., and Olweus, J. (2019). Induction of neoantigen-reactive T cells from healthy donors. Nat. Protoc. *14*, 1926–1943.
17. Rollins, M.R., Spartz, E.J., and Stromnes, I.M. (2020). T Cell Receptor Engineered Lymphocytes for Cancer Therapy. Curr. Protoc. Immunol. *129*, e97.
18. Pauwels, K., Gijsbers, R., Toelen, J., Schambach, A., Willard-Gallo, K., Verheust, C., Debyser, Z., and Herman, P. (2009). State-of-the-art lentiviral vectors for research use: risk assessment and biosafety recommendations. Curr. Gene Ther. *9*, 459–474.
19. Zhang, J., Hu, Y., Yang, J., Li, W., Zhang, M., Wang, Q., Zhang, L., Wei, G., Tian, Y., Zhao, K., et al. (2022). Non-viral, specifically targeted CAR-T cells achieve high safety and efficacy in B-NHL. Nature *609*, 369–374.
20. Green, M.L., Leisenring, W., Xie, H., Mast, T.C., Cui, Y., Sandmaier, B.M., Sorror, M.L., Goyal, S., Özkök, S., Yi, J., et al. (2016). Cytomegalovirus viral load and mortality after haemopoietic stem cell transplantation in the era of pre-emptive therapy: a retrospective cohort study. Lancet Haematol. *3*, e119–e127.
21. Tan, A.T., Meng, F., Jin, J., Zhang, J.Y., Wang, S.Y., Shi, L., Shi, M., Li, Y., Xie, Y., Liu, L.M., et al. (2022). Immunological alterations after immunotherapy with short lived HBV-TCR T cells associates with long-term treatment response in HBV-HCC. Hepatol. Commun. *6*, 841–854.
22. Kah, J., Koh, S., Volz, T., Ceccarello, E., Allweiss, L., Lütgehetmann, M., Bertoletti, A., and Dandri, M. (2017). Lymphocytes transiently expressing virus-specific T cell receptors reduce hepatitis B virus infection. J. Clin. Invest. *127*, 3177–3188.
23. Pei, X.Y., Zhao, X.Y., Liu, X.F., Mo, X.D., Lv, M., Xu, L.P., Wang, Y., Chang, Y.J., Zhang, X.H., Liu, K.Y., and Huang, X.J. (2022). Adoptive therapy with cytomegalovirus-specific T cells for cytomegalovirus infection after haploidentical stem cell transplantation and factors affecting efficacy. Am. J. Hematol. *97*, 762–769.
24. Liu, G., Chen, H., Cao, X., Jia, L., Rui, W., Zheng, H., Huang, D., Liu, F., Liu, Y., Zhao, X., et al. (2022). Efficacy of pp65-specific TCR-T cell therapy in treating cytomegalovirus infection after hematopoietic stem cell transplantation. Am. J. Hematol. *97*, 1453–1463.
25. Foy, S.P., Jacoby, K., Bota, D.A., Hunter, T., Pan, Z., Stawiski, E., Ma, Y., Lu, W., Peng, S., Wang, C.L., et al. (2023). Non-viral precision T cell receptor replacement for personalized cell therapy. Nature *615*, 687–696.
26. Nahmad, A.D., Reuveni, E., Goldschmidt, E., Tenne, T., Liberman, M., Horovitz-Fried, M., Khosravi, R., Kobo, H., Reinstein, E., Madi, A., et al. (2022). Frequent aneuploidy in primary human T cells after CRISPR-Cas9 cleavage. Nat. Biotechnol. *40*, 1807–1813.
27. Takenaka, K., Nishida, T., Asano-Mori, Y., Oshima, K., Ohashi, K., Mori, T., Kanamori, H., Miyamura, K., Kato, C., Kobayashi, N., et al. (2015). Cytomegalovirus Reactivation after Allogeneic Hematopoietic Stem Cell Transplantation is Associated with a Reduced Risk of Relapse in Patients with Acute Myeloid Leukemia Who Survived to Day 100 after Transplantation: The Japan Society for Hematopoietic Cell Transplantation Transplantation-related Complication Working Group. Biol. Blood Marrow Transpl. *21*, 2008–2016.
28. Saez-Ibañez, A.R., Upadhaya, S., Partridge, T., Shah, M., Correa, D., and Campbell, J. (2022). Landscape of cancer cell therapies: trends and real-world data. Nat. Rev. Drug Discov. *21*, 631–632.
29. Mhaidly, R., and Verhoeyen, E. (2019). The Future: In Vivo CAR T Cell Gene Therapy. Mol. Ther. *27*, 707–709.
30. Rurik, J.G., Tombácz, I., Yadegari, A., Méndez Fernández, P.O., Shewale, S.V., Li, L., Kimura, T., Soliman, O.Y., Papp, T.E., Tam, Y.K., et al. (2022). CAR T cells produced in vivo to treat cardiac injury. Science *375*, 91–96.
31. Foster, J.B., Griffin, C., Rokita, J.L., Stern, A., Brimley, C., Rathi, K., Lane, M.V., Buongervino, S.N., Smith, T., Madsen, P.J., et al. (2022). Development of GPC2-directed chimeric antigen receptors using mRNA for pediatric brain tumors. J. Immunother. Cancer *10*, e004450.

YMTHE, Volume *32*

Supplemental Information

Circular mRNA-based TCR-T offers a safe and effective therapeutic strategy for treatment of cytomegalovirus infection

Lianghua Shen, Jiali Yang, Chijian Zuo, Jian Xu, Ling Ma, Qiaomei He, Xiao Zhou, Xiaodan Ding, Lixiang Wei, Suqin Jiang, Luanluan Ma, Benjia Zhang, Yuqin Yang, Baoxia Dong, Liping Wan, Xueying Ding, Ming Zhu, Zhenhua Sun, Pengran Wang, Xianmin Song, and Yan Zhang

Supplemental Information

Supplemental figures and legends

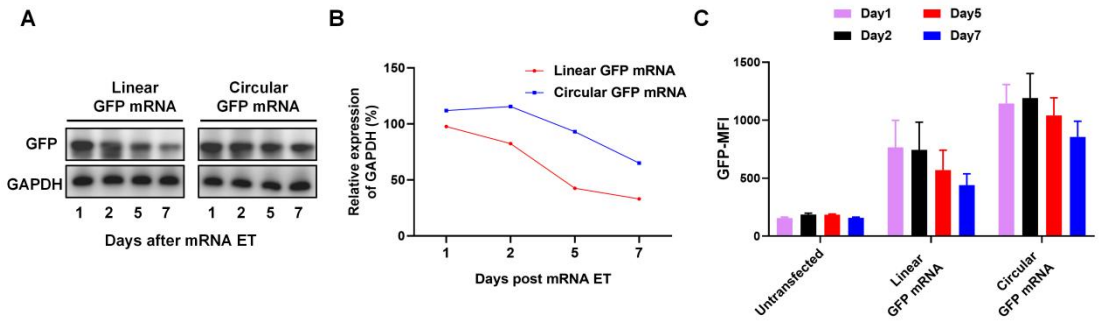

Fig. S1: Comparison of the protein expression level and MFI of circular mRNA and linear mRNA. (A) GFP expression on days 1, 2, 5, 7 after DC electroporation of linear or circular GFP mRNA by Western blot. (B) GFP protein expression relative to GAPDH was calculated by gray-scale measurements. (C) Comparison of GFP-MFI on day 1, 2, 5, 7 after circular or linear GFP-mRNA electroporation, the GFP-MFI values were quantified based on the whole population, n=3.

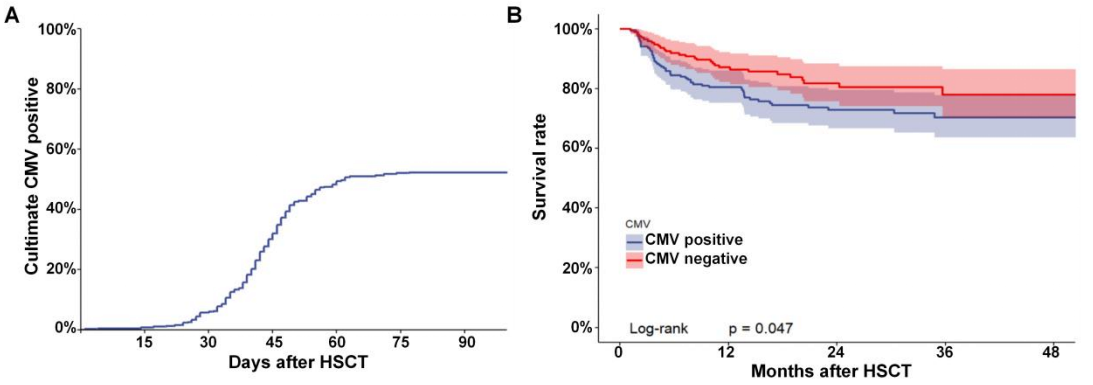

Days after HSCT (*N*=389)	
CMV infection	*N*=208 (53.5%)
No CMV infection	*N*=181 (46.5%)
Median number of days of CMV infection	56.1
Median copy number of CMV infection	327710

Death after HSCT (*N*=389)	
CMV positive (*N*=208)	CMV negative(*N*=181)
53 (25.7%)	31 (17.7%)
Log-rank	*p*=0.047

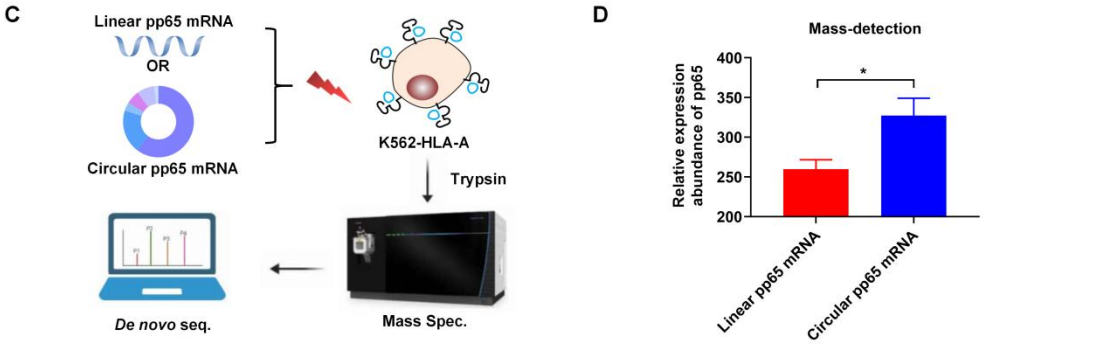

E

HLA-A*02:01-restricted pp65-TCR

ID	CDR3s	Frequency	Proportion(%)
1	TRB:CASSLEGYTEAFF TRA:CAFPYNNNDMRF TRA:CLLGERYGGSQGNLIF	14559	99.64
2	TRB:CATSTETGEAFF TRA:CAVNGAGSYQLTF	19	0.13
3	TRB:CASRTTTGVRTDTQYF TRA:CAFPYNNNDMRF TRA:CAPFGNAGNMLTF	16	0.11
4	TRB:CASRGGGTQPWDEQFF TRA:CARNTGNQFYF	6	0.04
5	TRB:CAWSSRGAMTDTQYF TRA:CAEYTGTASKLTF	3	0.02
6	TRA:CAVGFGNQFYF	1	0.01
7	TRB:CASSLEGYTEAFF	1	0.01
8	TRB:CASSYFGSHDEQFF TRA:CAATNAGGTSYGKLTF	1	0.01
9	TRA:CAFPYNNNDMRF	1	0.01
10	TRA:CAFPYNNNDMRF	1	0.01

F

HLA-A*11:01-restricted pp65-TCR

ID	CDR3s	Frequency	Proportion(%)
1	TRB:CASSSTRGPGNQPQHF TRA:CAYRSFYTGANSKLTF	8582	80.96
2	TRB:CASSVAVRGEETQYF TRA:CAMSVYNAGNMLTF	788	7.43
3	TRB:CASSFFRGEGNQPQHF TRB:CASSSFRGEGNQPQHF TRA:CAYRSFYTGANSKLTF	591	5.58
4	TRB:CASSVAVRGEETQYF TRB:CASSVSGWGPQETQYF TRA:CATDNSGAGSYQLTF	97	0.92
5	TRB:CASSLSAVEDYEQYF TRA:CLASGNTGKLIF	88	0.83
6	TRB:CASSFFRGEGNQPQHF	65	0.61
7	TRB:CASSLQREGKNIQYF TRA:CAMRLPFNNAGNMLTF	41	0.39
8	TRB:CASSTLREPYNEQFF TRA:CAVHPMQAGTALIF	38	0.36
9	TRB:CASSVAVRGEETQYF	28	0.26
10	TRB:CASRRGLSKTTEAFF TRA:CAVTDDTGKLIF	15	0.14

G

HLA-A*24:02-restricted pp65-TCR

ID	CDR3s	Frequency	Proportion(%)
1	TRB:CAISDPGSSFGGYTF TRA:CARSNYGGSQGNLIF	1510	74.17
2	TRB:CASSSNQGNTIYF TRA:CAFGTYKYIF	136	6.68
3	TRB:CASSLVLAPDEQFF TRA:CARNAGNMLTF	139	6.43
4	TRB:CASSDRSTTDTQYF TRA:CARYTDKLIF	105	5.16
5	TRB:CASRRGLSKTTEAFF TRA:CAVTDDTGKLIF	12	0.59
6	TRB:CASSFTGTPKFF TRA:CASPSGNTGKLIF	9	0.44
7	TRB:CASSLVEQGHFYEQYF TRB:CASSRGRPLQYF TRA:CLVGERNAGNMLTF	4	0.20
8	TRB:CAWSTGTVSSYEQYF TRA:CAMREGHQFYF	3	0.15
9	TRB:CASSLYGTLNTEAFF TRA:CAVNGGGSNYKLTF	2	0.10
10	TRB:CASSLAGSGFGEQFF TRA:CVVSARNAGNNRKLIW	2	0.10

Fig. S2: CMV clinical data analysis and CMV-pp65-TCR single-cell sequencing. (A) CMV incidence and median time after HSCT in Shanghai General Hospital from 2018-2021. (B) Survival curve analysis of the impact of CMV infection on patient survival after HSCT. (C) General overview of trypsin digestion and mass

spectrometry sequencing experiments. (D) Mass spectrometry sequencing analysis of pp65 protein relative expression abundance per two million target cell, *n*=3, "*" mean *P*<0.05, (E-G) After single-cell TCR sequencing, the HLA-A*02:01/ A*11:01/A*24:02-restricted TCRs were sorted by clonetypes according to frequency, respectively.

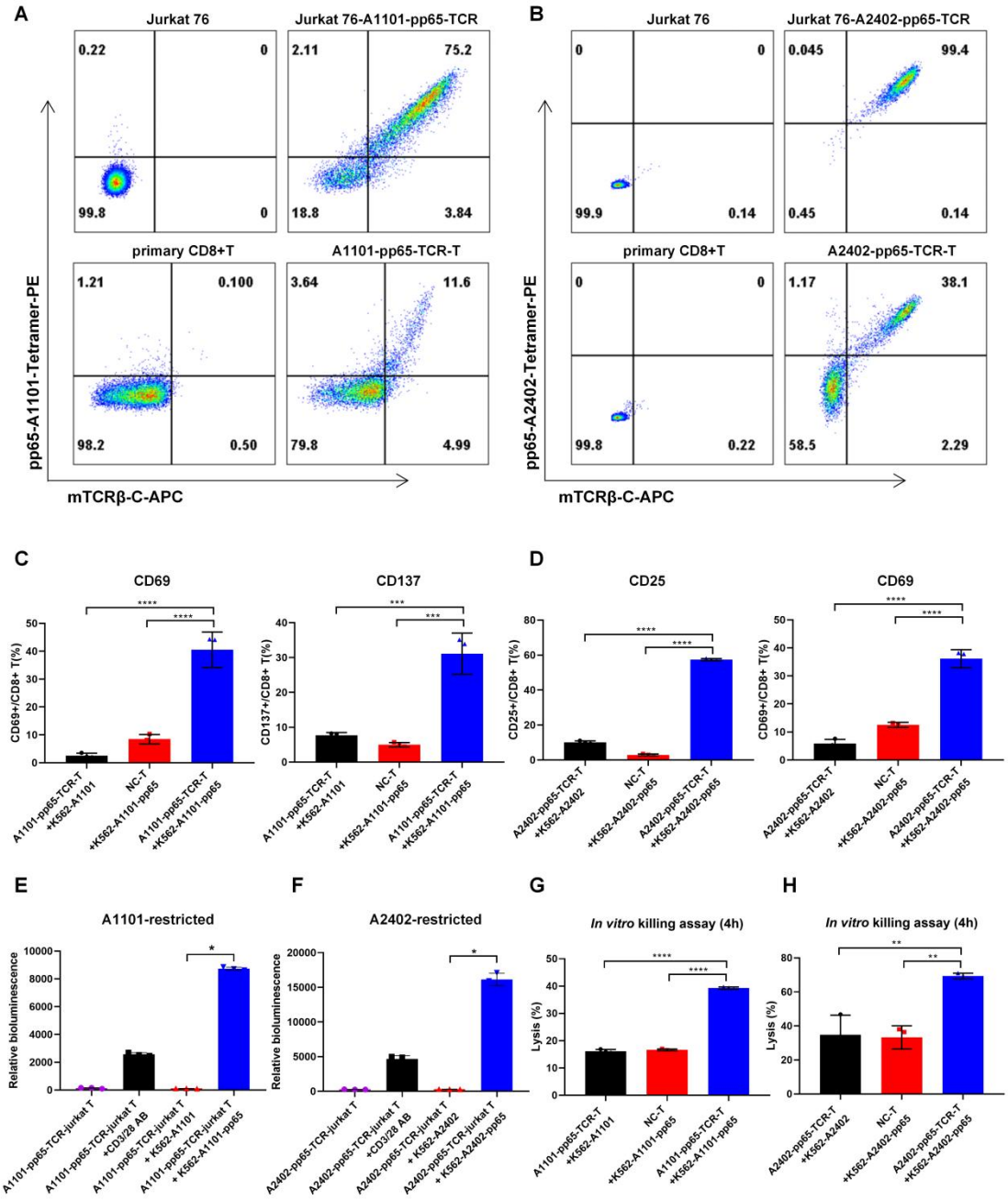

Fig. S3: Identification of the function of HLA-A*11:01/A*24:02 restricted pp65-TCR. (A-B) *In vitro* binding assay validation using HLA-A*11:01 or HLA-A*24:02 tetramer after pp65-TCR lentivirus infection of Jurkat 76-CD8 cells and primary $CD8^+$ T cells. (C) Flow cytometry was performed to detect the expression levels of activation-related markers (CD69 and CD137) after co-culture of HLA-A*11:01-restricted pp65-TCR-T cells with control cells or target cells. (D) Flow

cytometry was performed to detect the expression levels of activation-related markers (CD25 and CD69) after co-culture of HLA-A*24:02-restricted pp65-TCR-T cells with control cells or target cells. (E-F) Jurkat T-NFAT-Luciferase reporter system detects the activation level of HLA-A*11:01 or HLA-A*24:02 restricted pp65-TCR-T after co-culture with control or target cells. A non-parametric test is used and will be compared using the Friedman test. n=3, "*" mean P<0.05. (G-H) Flow cytometry was used to detect the killing efficiency of HLA-A*11:01 or HLA-A*24:02 restricted pp65-TCR-T after co-culture with control or target cells at E:T=1:1. All data represent the mean ± SEM. n=3, "**" mean P<0.01, "***" mean P<0.001, "****" mean P<0.0001.

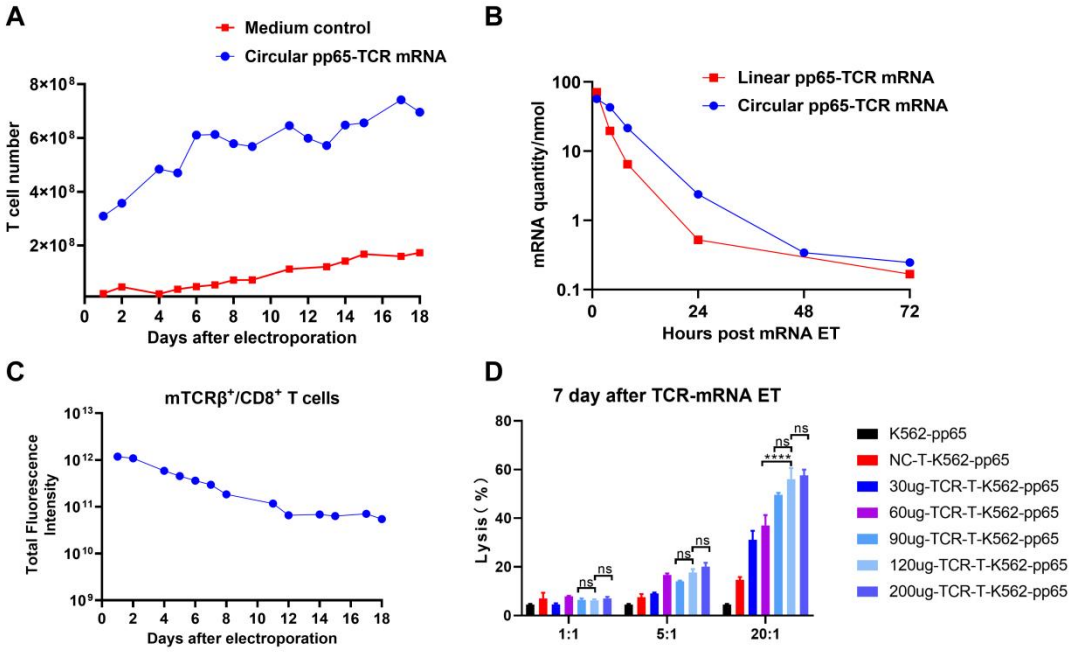

Fig. S4: *In vitro* expression and killing ability assay of pp65-TCR cmRNA. (A) Dynamic changes in T-cell numbers within 18 days after electroporation. (B) Determined quantity of linear or circular pp65-TCR mRNA by qPCR. (C) Total fluorescence intensity of all cells within 18 days after T cell electrotransfer of pp65-TCR cmRNA. (D) After cm-pp65-TCR-T co-culture with control or target cells at different E:T or different dose of cmRNA for 4 h, killing efficiency were observed when the cm-pp65-TCR-T cells 7 day after electroporation. Data represent the mean ± SEM. *n*=3, "****" mean *P*<0.0001.

Supplemental table

Table S1: Flow Cytometry antibodies information

mAb	Conj	Clone	Cat#	Supplier
Human CD3	PE-Cy7	HIT3a	300316	Biolegend
Human CD8a	APC	SK1	317317	Biolegend
Human CD8a	BV421	SK1	344747	Biolegend
pp65-HLA-A*02:01-Tetramer	PE	NLVPMVATV	TB-0010-1	MBL Biotech.
pp65-HLA-A*11:01-Tetramer	PE	ATVQGQNLK	TB-M012-1	MBL Biotech.
pp65-HLA-A*24:02-Tetramer	PE	QYDPVAALF	TS-0020-1C	MBL Biotech.
Mouse TCRβ-C	APC	H57-597	109212	Biolegend
Human CD25	BV421	BC96	302629	Biolegend
Human CD69	PE	FN50	310905	Biolegend
Human CD137	PE-Cy7	DREG-56	304834	Biolegend
Human IFN-γ	APC	4S.B3	80811-80	Biogems Biotech.
Human IFN-γ	PE	B27	554701	BD pharmingen
Human TNF-α	APC	MAb11	502912	Biolegend
Human TNF-α	PE-Cy7	MAb11	557647	BD pharmingen
Human GZMB	FITC	QA16A02	372205	Biolegend
Human CD107a	PE	H4A3	555801	BD pharmingen
Celltrace Violet	BV421		C34557	Thermo
Live/dead eFluor780	eF780		65-0865	Thermo